



# University of HUDDERSFIELD

## University of Huddersfield Repository

Okorji, Uchechukwu P., Velagapudi, Ravikanth, El-Bakoush, Abdelmeneim, Fiebich, Bernd L. and Olajide, Olumayokun A.

Antimalarial drug artemether inhibits neuroinflammation in BV2 microglia through Nrf2-dependent mechanisms

### Original Citation

Okorji, Uchechukwu P., Velagapudi, Ravikanth, El-Bakoush, Abdelmeneim, Fiebich, Bernd L. and Olajide, Olumayokun A. (2015) Antimalarial drug artemether inhibits neuroinflammation in BV2 microglia through Nrf2-dependent mechanisms. *Molecular Neurobiology*, 53 (9). pp. 6426-6443. ISSN 1559-1182

This version is available at <http://eprints.hud.ac.uk/id/eprint/26513/>

The University Repository is a digital collection of the research output of the University, available on Open Access. Copyright and Moral Rights for the items on this site are retained by the individual author and/or other copyright owners. Users may access full items free of charge; copies of full text items generally can be reproduced, displayed or performed and given to third parties in any format or medium for personal research or study, educational or not-for-profit purposes without prior permission or charge, provided:

- The authors, title and full bibliographic details is credited in any copy;
- A hyperlink and/or URL is included for the original metadata page; and
- The content is not changed in any way.

For more information, including our policy and submission procedure, please contact the Repository Team at: [E.mailbox@hud.ac.uk](mailto:E.mailbox@hud.ac.uk).

<http://eprints.hud.ac.uk/>

**Antimalarial drug artemether inhibits neuroinflammation in BV2 microglia through Nrf2-dependent mechanisms**

**Uchechukwu P Okorji<sup>1#</sup>, Ravikanth Velagapudi<sup>1#</sup>, Abdelmeneim El-Bakoush<sup>1</sup>, Bernd L Fiebich<sup>2, 3</sup>, Olumayokun A Olajide<sup>1\*</sup>**

<sup>1</sup> Department of Pharmacy, School of Applied Sciences, University of Huddersfield Queensgate, Huddersfield, West Yorkshire, HD1 3DH, United Kingdom

<sup>2</sup> Neurochemistry Research Laboratory, Department of Psychiatry and Psychotherapy, University of Freiburg Medical School, Hauptstrasse 5, 79104 Freiburg, Germany

<sup>3</sup> VivaCell Biotechnology GmbH, Ferdinand-Porsche-Str. 5, D-79211, Denzlingen, Germany

**\*Author for Correspondence:**

Dr Olumayokun Olajide  
Department of Pharmacy  
University of Huddersfield  
Queensgate  
Huddersfield, HD1 3DH  
United Kingdom

Email: [o.a.olajide@hud.ac.uk](mailto:o.a.olajide@hud.ac.uk)

Telephone: +44 (0) 1484 472735

**# contributed equally to the study**

## Abstract

Artemether, a lipid-soluble derivative of artemisinin has been reported to possess anti-inflammatory properties. In this study, we have investigated the molecular mechanisms involved in the inhibition of neuroinflammation by the drug. The effects of artemether on neuroinflammation-mediated HT22 neuronal toxicity were also investigated in a BV2 microglia/HT22 neuron co-culture. To investigate effects on neuroinflammation, we used LPS-stimulated BV2 microglia treated with artemether (5-40 $\mu$ M) for 24 hours. ELISAs and western blotting were used to detect pro-inflammatory cytokines, nitric oxide, PGE<sub>2</sub>, iNOS, COX-2 and mPGES-1. BACE-1 activity and A $\beta$  levels were measured with ELISA kits. Protein levels of targets in NF- $\kappa$ B and p38 MAPK signalling, as well as HO-1, NQO1 and Nrf2 were also measured with western blot. NF- $\kappa$ B binding to the DNA was investigated using EMSA. MTT, DNA fragmentation and ROS assays in BV2-HT22 neuronal co-culture were used to evaluate the effects of artemether on neuroinflammation-induced neuronal death. The role of Nrf2 in the anti-inflammatory activity of artemether was investigated in BV2 cells transfected with Nrf2 siRNA. Artemether significantly suppressed pro-inflammatory mediators (NO/iNOS, PGE<sub>2</sub>/COX-2/mPGES-1, TNF $\alpha$ , and IL-6), A $\beta$  and BACE-1 in BV2 cells following LPS stimulation. These effects of artemether were shown to be mediated through inhibition of NF- $\kappa$ B and p38MAPK signalling. Artemether produced increased levels of HO-1, NQO1 and GSH in BV2 microglia. The drug activated Nrf2 activity by increasing nuclear translocation of Nrf2 and its binding to antioxidant response elements in BV2 cells. Transfection of BV2 microglia with Nrf2 siRNA resulted in the loss of both anti-inflammatory and neuroprotective activities of artemether. We conclude that artemether induces Nrf2 expression and suggest that Nrf2 mediates the anti-inflammatory effect of artemether in BV2 microglia. Our results suggest that this drug has a therapeutic potential in neurodegenerative disorders.

**Keywords**

Artemether, neuroinflammation, BV2 microglia, HT22 hippocampal neurons, NF- $\kappa$ B, Nrf2

Accepted Manuscript

## 1 Background

In the central nervous system (CNS), the microglia plays an important role in immune defence and tissue repair [1]. Under normal conditions, these cells provide surveillance whilst maintaining homeostasis in the brain [2]. In response to injury, harmful toxins, infection or inflammation, microglial cells become activated, secreting pro-inflammatory mediators such as nitric oxide (NO), prostaglandin E<sub>2</sub> (PGE<sub>2</sub>), reactive oxygen/nitrogen species and pro-inflammatory cytokines including IL-6 and TNF $\alpha$  [3, 4]. These pro-inflammatory mediators are mainly regulated by the transcription factor NF- $\kappa$ B [5]. NF- $\kappa$ B binds to the DNA and its transcriptional activity regulates several genes, which promote neuroinflammation. The p38 mitogen-activated protein kinase (p38 MAPK) signalling pathway also plays an important role in the expression and activity of pro-inflammatory cytokines in microglial cells [6-8].

Excessive production of pro-inflammatory mediators generated during neuroinflammation can damage neighbouring neurons, and further activate the microglia, as well as other glia cells resulting in a self-perpetuating cycle [2, 4, 9]. Furthermore, activation of the microglia and the resulting neuroinflammation play a critical role in the pathogenesis of neurodegenerative disorders such as Alzheimer's disease (AD) [10]. Consequently, pharmacological modulation of pro-inflammatory mediators generated by the microglia during chronic inflammation and modulation of the signalling pathways responsible for their production is an important target in treating severe neuroinflammatory disorders.

Neuroinflammation has been reported to play a major role in the formation of amyloid beta (A $\beta$ ) [11]. Studies have also shown that lipopolysaccharide (LPS) can stimulate A $\beta$  deposition [12-14], suggesting that neuroinflammation could be a causative contributor in the development and/or progression of AD.

Recently, interests have focused on the nuclear factor-erythroid 2-related factor 2 (Nrf2) signalling in antioxidant response element (ARE)-mediated regulation of gene expression. Nrf2 is a redox-sensitive transcription factor, which on activation under oxidant conditions binds to the ARE promoter and activates a battery of antioxidant and cytoprotective genes that include heme oxygenase-1 (HO-1). Nrf2 and its target genes modulate microglial phenotype, restore redox homeostasis and attenuate pro-inflammatory phenotype in favour of anti-inflammatory phenotypes [15]. In a study

using HO-1 knockout mice, Kapturczak et al (2004) showed that a pro-inflammatory tendency was associated with HO-1 deficiency [16]. Hence, pharmacological induction of HO-1 via Nrf2 pathway might be an important strategy in modulating neuroinflammation. Considering the protective effects of Nrf2 against oxidative injury, recent studies have also implicated Nrf2 in neuroprotection [17, 18].

Artemether (Figure 1) is the lipid-soluble derivative of artemisinin [19]. Although currently used in the treatment of malaria, experiments on experimental rheumatoid arthritis have shown that artemether could be offered as a second-line drug treatment of rheumatoid arthritis [20]. In addition, artemether has been shown to have anti-inflammatory effects in a mouse model of colitis [21]. In spite of studies showing anti-inflammatory potentials of artemether, we do not know whether this drug could interfere with signalling pathways involved in neuroinflammation in LPS-activated microglia. Therefore, in this study, we have investigated the effects of artemether on neuroinflammation in LPS-activated BV2 microglial cells. We also investigated the effect of artemether on neuroinflammation-induced neurotoxicity in HT22 cells co-cultured with BV2 microglia. The roles of Nrf2/HO-1 activation on the anti-inflammatory and neuroprotective effects of artemether were further investigated.

## **2. Methods**

### **2.1. Cell culture**

BV2 mouse microglia cell line ICLC ATL03001 (Interlab Cell Line Collection, Banca Biologica e Cell Factory, Italy) were maintained in RPMI 1640 medium with 10% fetal bovine serum (FBS) (Sigma), 2 mM L-glutamine (Sigma), 100 U/ml penicillin and 100 mg/ml streptomycin (Sigma) in a 5 % CO<sub>2</sub> incubator.

HT22 mouse hippocampal cells were cultured in DMEM supplemented with 10 % FBS, 100 U/ml penicillin and 100 µg/ml streptomycin in a 5 % CO<sub>2</sub> incubator at 37°C.

### **2.2. Drugs and treatment**

Artemether (Sigma) was dissolved in dimethyl sulphoxide (DMSO) to a concentration of 0.1 M and aliquots stored in -80°C. BAY 11-7085 and SKF 86002 dihydrochloride were purchased from Tocris. In all experiments, cells were treated with artemether (5-40 µM) in the absence or presence of LPS (1 µg/ml).

### **2.3. BV2 microglia viability assay**

The colorimetric 3-(4, 5-dimethylthiazol-2-yl)-2, 5-diphenyl tetrazolium bromide (MTT) assay was performed to determine the viability of BV2 microglia incubated with or without LPS (1 µg/ml) in the presence of artemether (5-40 µM) for 24 h.

Following drug treatment and stimulation with LPS, 200 µl MTT solution (5 mg/ml) was added to cells and incubated at 37 °C for 4 h. Thereafter, 200 µl of medium was removed from each well without disturbing the cell clusters, and 150 µl of DMSO solution added to wells to dissolve the formazan crystals. Thorough mixing of the preparation was facilitated by shaking the plate for a few seconds before absorbance was read at 540 nm with a plate reader (Infinite F50, Tecan).

### **2.4. Nitrite determination**

BV2 cells were seeded out ( $2 \times 10^5$  cells/ml) and cultured for 48 h. Thereafter cells were pre-treated with artemether (5-40 µM) for 30 min and stimulated with LPS for 24 h. Levels of nitrite in culture media were measured using commercially available Griess assay kit (Promega) according to manufacturer's instructions. Absorbance was measured at 540 nm in a microplate reader (Infinite F50, Tecan).

### **2.3. Determination of PGE<sub>2</sub> production in BV2 microglia**

BV2 cells were seeded out ( $2 \times 10^5$  cells/ml) and cultured in 96-well plates for 48 h. Thereafter, cells were pre-treated with artemether (5-40 µM) for 30 min and stimulated with LPS for 24 h. Levels of PGE<sub>2</sub> in culture medium were measured using commercially available enzyme immunoassay kit (Arbor Assays, Ann Arbor, Michigan, USA) according to manufacturer's instructions. Absorbance was measured at 450 nm in a microplate reader (Infinite F50, Tecan).

### **2.4. Determination of TNFα and IL-6 production in BV2 microglia**

Cultured BV2 microglia were pre-treated with artemether (5-40 µM) prior to stimulation with LPS (1 µg/ml). Twenty-four hours after stimulation, culture supernatants were collected and centrifuged. Concentrations of TNFα and IL-6 were measured with commercially available ELISA kits (BioLegend, UK), followed by measurements in a plate reader at a wavelength of 450 nm.

## **2.5. Reporter gene assays**

At confluence, cultured BV2 microglia were sub-cultured (at a ratio of 1:3) 24 h before transfection. Thereafter, cells were harvested and re-suspended at  $4 \times 10^5$  cells/ml in Opti-MEM containing 5% FBS. Cells were then seeded out in a solid white 96-well plate and incubated with pGL4.32[luc2P/NF- $\kappa$ B-RE/Hygro] vector (Promega, UK), using Fugene 6 (Promega) transfection reagent and incubated for a further 16 h at 37°C. Following transfection, media was changed to OPTI-MEM and incubated for a further 8 h. Thereafter, transfected cells were treated with artemether (5-40  $\mu$ M) or BAY 11-7085 (10  $\mu$ M) and incubated for 30 min at 37°C followed by LPS (1  $\mu$ g/ml) for 6 h. At the end of the stimulation, NF- $\kappa$ B-mediated gene expression was measured with One-Glo luciferase assay kit (Promega), according to the manufacturer's instructions.

To carry out the ARE-dependent reporter gene assay, BV2 microglia were seeded out and incubated in solid white 96-well at 37°C for 24 h. A transfection cocktail was made by diluting ARE vector (pGL4.37 [luc2P/ARE/Hygro]; Promega) at a concentration of 1 ng DNA/ $\mu$ l in Fugene 6 transfection reagent. The cocktail was incubated at room temperature for 20 min, and 8  $\mu$ l to each well, followed by incubation for 18 h at 37°C. Thereafter, culture medium was changed to OPTI-MEM and incubated for 6 h at 37°C. Cells were then treated with artemether (5-40  $\mu$ M) and incubated at 37°C for 8 h. Following incubation, plates were allowed to cool at room temperature for 15 min. Thereafter, 80  $\mu$ l of luciferase buffer containing luminescence substrate was added to each well and luminescence read with FLUOstar OPTIM reader (BMG LABTECH).

## **2.6. Isolation of nuclear extracts**

Nuclear extracts were prepared for experiments involving nuclear proteins, and was carried using a nuclear extraction kit (Abcam), according to the manufacturer's instructions.

## **2.7. Western blot**

Cytoplasmic protein extraction was performed on cells lysed in RIPA buffer containing 2 mM phenylmethylsulfonyl fluoride (PMSF) (Sigma). Lysates were centrifuged, and collected. Cell lysate (20  $\mu$ g) were separated by SDS-PAGE, blotted onto polyvinylidene difluoride (pvdf) membrane (Millipore). Transferred proteins were

incubated with the following primary antibodies at 4°C: anti-rabbit iNOS (1:500, Santa Cruz), rabbit anti-COX-2 (1:500; Santa Cruz), rabbit anti-mPGES-1 (1:1000; Agri Sera), rabbit anti-phospho-p38 (1:250; Santa Cruz), rabbit anti-phospho-MAPKAPK2 (1:200; Assay Biotechnology), rabbit anti-phospho- MKK3/6 (1:1000; Santa Cruz), rabbit phospho-I $\kappa$ B $\alpha$  (1:250; Santa Cruz, rabbit phospho-p65 NF- $\kappa$ B (1:500; Santa Cruz), rabbit HO-1 (1:1000; Santa Cruz), rabbit Nrf2 (1:500; Santa Cruz), rabbit NQO1 (1:500; Santa Cruz) and rabbit anti-actin (1:1000; Sigma). After extensive washing (three times for 15 min each in TBS-T), proteins were detected by incubation with Alexa Fluor 680 goat anti-rabbit secondary antibody (1:10000; Life Technologies) at room temperature for 1 h. Detection was done using a LICOR Odyssey Imager.

## **2.8. Immunofluorescence**

Microglia cells were cultured in 24 well plates. At confluence, cells were pre-treated with artemether (5-40  $\mu$ M) for 30 min followed by LPS (1  $\mu$ g/ml) stimulation for 60 min (NF- $\kappa$ B) and 24 h (Nrf2 activation). Cells were fixed with ice-cold 100% methanol for 15 min at -20°C and later washed 3 times for 5 min with PBS. Non-specific binding sites were blocked by incubating cells in 5% BSA blocking solution (containing 10% horse serum in 1X TBS-T) for 60 min at room temperature followed by washing with PBS. Thereafter, the cells were incubated with rabbit anti-NF- $\kappa$ B p65 (Santa Cruz; 1:100) antibody or anti-Nrf2 (Santa Cruz; 1:100) overnight at 4°C. Following overnight incubation, cells were washed 3 times with PBS and incubated for 2 h in dark with Alexa Fluor 488-conjugated donkey anti-rabbit IgG (Life Technologies; 1:500) secondary antibody. Thereafter, cells were washed with PBS and counterstained with 4', 6 diamidino-2-phenylindole dihydrochloride (50 nm, DAPI; Invitrogen) for 5 min. After rinsing cells with PBS, excess buffer was removed and gold antifade reagent (Invitrogen) was added. All staining procedures were performed at room temperature. Representative fluorescence images were obtained using EVOS<sup>®</sup> FLoid<sup>®</sup> cell imaging station.

## **2.9. Electrophoretic mobility shift assays (EMSA)**

An ELISA-based DNA binding assay (EMSA) was used to investigate the effects of artemether on DNA binding of NF- $\kappa$ B. BV2 microglia were treated with 5, 10, 20 and 40  $\mu$ M artemether or BAY 11-7085 (10  $\mu$ M). Thirty minutes later, cells were

stimulated with LPS (1 µg/ml). After 1 h, nuclear extracts were prepared using EpiSeeker Nuclear Extraction Kit (Abcam), according to the manufacturer's instructions. DNA binding assay was carried on nuclear extracts using the TransAM NF-κB transcription factor EMSA kit (Activ Motif, Belgium) according the manufacturer's instructions. The EMSA kit employs a 96-well plate to which an oligonucleotide containing the NF-κB consensus site (5' GGGACTTTCC-3') has been immobilised. Briefly, 30 µl of complete binding buffer were added to each well, followed by 20 µg nuclear extract samples. The plate was covered and rocked (100 rpm) for 1 h at room temperature. This was followed by addition of NF-κB antibody (1:1000; 1 h) and HRP-conjugated antibody (1:1000; 1 h). Absorbance was read on a Tecan F50 microplate reader at 450 nm.

To investigate DNA binding of Nrf2, BV2 microglia were treated with artemether (5-40 µM). Nuclear extracts were added to 96-well plates on which has been immobilised oligonucleotide containing the ARE consensus binding site (5' GTCACAGTGACTCAGCAGAATCTG-3'). Assay procedure was as described for NF-κB, using an Nrf2 antibody (1:1000; 1 h).

#### **2.10. GSH-Glo™ glutathione assay in BV2 microglia**

BV2 microglia were cultured in a 96-well plate ( $2 \times 10^5$  cells/ml). After 48 h, culture medium was changed to phenol red- and serum-free medium, treated with artemether (5-40 µM) and incubated for 24 h. At the end of the experiment, culture medium was removed and levels of GSH determined using GSH-Glo™ glutathione assay kit (Promega, Southampton), according to the manufacturer's instruction. Briefly, 100 µl of 1X GSH-Glo™ reagent was added to each well and incubated with shaking at room temperature for 30 min. Thereafter, 100µl of luciferin detection reagent was added to each well and incubated with shaking at room temperature for 15 min. Luminiscence was then read with with FLUOstar OPTIM reader (BMG LABTECH).

#### **2.11. Determination of Aβ and BACE-1 in LPS activated BV2 microglia**

To investigate the effect of artemether on Aβ and BACE-1 production BV2 cells were pre-treated with artemether (5-40 µM) followed by stimulation with LPS (1 µg/ml) for 24 h. Thereafter, cell culture supernatants were collected, centrifuged and analysed for Aβ and BACE-1 using Aβ and BACE-1 ELISA kits (Life Technologies).

### **2.12. BV2 microglia/HT22 mouse hippocampal neuron co-culture**

Neuroprotective effects of artemether were investigated using a transwell co-culture system. BV2 cells were cultured at a density of  $5 \times 10^4$  on transwell inserts (pore size  $0.4 \mu\text{m}$ ; Corning) in 96-well plate placed above the HT22 neuronal layer.

### **2.13. Determination of HT22 cell viability**

The effect of microglial activation on HT22 neuron viability was measured using the MTT assay. Twenty-four hours after establishing co-culture, BV2 cells were pre-treated with artemether ( $5\text{-}40 \mu\text{M}$ ) and then stimulated with LPS ( $1 \mu\text{g/ml}$ ) for 24 h. After the experiment,  $200 \mu\text{l}$  MTT solution ( $5 \text{mg/ml}$ ) was added to each well containing HT22 neurons and incubated at  $37^\circ\text{C}$  for 4 h. Then,  $200 \mu\text{l}$  of medium was removed from each well without disturbing the cell clusters, and  $150 \mu\text{l}$  of DMSO solution added to wells to dissolve the formazan crystals. Thorough mixing of the preparation was facilitated by shaking the plate for a few seconds before absorbance was read at  $540 \text{nm}$  with a plate reader.

### **2.14. Measurement of Intracellular ROS production**

The effect of microglial activation on intracellular ROS levels in HT22 cells was performed using the fluorescent 2',7'-dichlorofluorescein diacetate DCFDA-cellular reactive oxygen species detection assay kit (Abcam). Twenty-four hours after establishing transwell co-culture, HT22 neurons were incubated with  $10 \mu\text{M}$  DCFDA for 30 min at  $37^\circ\text{C}$ . After removal of excess DCFDA, HT22 cells were washed and the microglial layer pre-treated with artemether ( $5\text{-}40 \mu\text{M}$ ) for 30 min followed by stimulation with  $1 \mu\text{g/ml}$  LPS for 4 h at  $37^\circ\text{C}$ . Intracellular production of ROS was measured by the fluorescence detection of dichlorofluorescein (DCF) as the oxidised product of DCFH on a microplate reader with an excitation wavelength of  $485 \text{nm}$  and emission wavelength of  $535 \text{nm}$ .

### **2.15. Cellular DNA fragmentation assay**

The effect of microglial activation on cellular DNA fragmentation in HT22 cells was conducted using an assay kit (Roche Diagnostics, Mannheim, Germany), according to the manufacturer's instructions. HT22 neurons were co-cultured with BV2 cells grown in transwells. Thereafter, the neurons were labelled with 5-bromo-2'-deoxyuridine (BrdU) for 12 h. Following labelling, BV2 microglia were treated with

artemether (5-40  $\mu$ M) 30 min prior to stimulation with LPS for 24 h. Cells were centrifuged at 250 g for 10 min and supernatants removed. The cells were then lysed with 200  $\mu$ l of buffer and incubated for 30 min at room temperature. Cells were centrifuged again at 250 g for 10 min and supernatants removed. The labelled DNA in the supernatants as a result of DNA fragmentation was measured using ELISA with an anti-BrdU antibody.

### **2.16. Nrf2 siRNA transfections**

Small interfering RNA (siRNA) targeted at Nrf2 (Santa Cruz Biotechnology) was used to knockout Nrf2. BV2 cells were cultured and incubated at 37°C in a 5% CO<sub>2</sub> incubator until 70-80 % confluent. Thereafter, 2  $\mu$ l Nrf2 siRNA duplex were diluted into 100  $\mu$ l of siRNA transfection medium (Santa Cruz Biotechnology). In a separate tube, 2  $\mu$ l of transfection reagent (Santa Cruz biotechnology) was diluted into 100  $\mu$ l of siRNA transfection medium. The dilutions were mixed gently and incubated for 30 min at room temperature. Next, cells were incubated in Nrf2 siRNA transfection cocktail for 6 h at 37°C. Control BV2 microglia were transfected with control siRNA. Following transfection, media was changed in Nrf2 siRNA and control siRNA transfected cells to complete media and incubated for a further 18 h. Effects of artemether (40  $\mu$ M) on NO, PGE<sub>2</sub>, TNF $\alpha$  and IL-6 production in LPS-stimulated control siRNA and Nrf2-siRNA-transfected BV2 cells were then determined. NF- $\kappa$ B DNA binding assays were also conducted in LPS-stimulated control siRNA and Nrf2-siRNA-transfected BV2 cells treated with artemether (40  $\mu$ M). Transfection efficiency was determined by preparing nuclear extracts from both control siRNA and Nrf2-siRNA-transfected BV2 cells, and western blot carried out for levels of Nrf2 protein.

### **2.17. Statistical analysis**

Values of all experiments were represented as a mean  $\pm$  SEM of at least 3 experiments. Values were compared using one-way ANOVA followed by a post-hoc Student Newman-Keuls test.

### 3. Results

#### 3.1 Artemether treatment did not affect viability of BV2 microglia

BV2 cells were stimulated with LPS (1 µg/ml) in the presence or absence of artemether (5-40 µM) for 24 h. Subsequent determination of cell viability showed that there was no significant difference in cell viability with various treatments compared to the untreated cells (Figure 2).

#### 3.2 Artemether reduced iNOS-mediated NO production in LPS-stimulated microglial cells

In LPS treated BV2 cells, there was a marked increase in NO production, when compared to unstimulated cells. Pre-treatment with artemether (5-40 µM) significantly reduced ( $p < 0.01$ ) nitrite production in a concentration-dependent manner (Figure 3a). With 10 µM of the drug, nitrite production was 42.3 %. Subsequent increases in concentration from 20 µM to 40 µM resulted in ~1.2 fold decrease in nitrite production. Further investigations showed with the lowest concentration (5 µM), artemether did not significantly inhibit levels of iNOS protein. At 10 µM, there was a slight reduction in the level of iNOS protein. However, with an increase in concentration to 20 and 40 µM, artemether significantly ( $p < 0.001$ ) reduced levels of iNOS protein following LPS stimulation (Figure 3b).

#### 3.3 Artemether inhibited COX-2 and mPGES-1 mediated PGE<sub>2</sub> production in LPS-activated BV2 Microglia

The activation of BV2 microglia with LPS resulted in a significant increase in PGE<sub>2</sub> production compared to untreated control after 24 h stimulation (Figure 4a). However, when pre-treated with artemether (5, 10, 20 and 40 µM), there was a significant ( $p < 0.001$ ) reduction in the production of PGE<sub>2</sub> (Figure 4a). At 40 µM, PGE<sub>2</sub> release was reduced ~2.2-fold, compared with LPS control ( $p < 0.001$ ).

Following our observation that artemether reduced LPS-induced PGE<sub>2</sub> production, we investigated the effect of the drug on the levels of COX-2 and mPGES-1 proteins in LPS-stimulated BV2 microglia. Figure 4b shows that there was a marked increase in COX-2 protein in LPS-activated BV2 microglia. Pre-treatment with 5 µM artemether produced a modest effect on LPS-induced COX-2 protein expression. However, an increase in concentrations of the drug to 10, 20 and 40 µM resulted in

significant reduction of COX-2 protein (~ 1.3-fold,  $p < 0.001$  at 10  $\mu\text{M}$ ; ~1.4-fold,  $p < 0.001$  at 20  $\mu\text{M}$ ; ~1.7-fold,  $p < 0.001$  at 40  $\mu\text{M}$ ) (Figure 4b). In addition, artemether (5-40  $\mu\text{M}$ ) significantly ( $p < 0.001$ ) suppressed levels of mPGES-1 protein following LPS activation at all concentrations (Figure 4c). At 40  $\mu\text{M}$ , mPGES-1 expression was significantly reduced (~2.2-fold,  $p < 0.001$ ).

### **3.4 Artemether reduced the production of TNF $\alpha$ and IL-6**

Following stimulation of BV2 microglia with LPS (1  $\mu\text{g/ml}$ ), levels of TNF $\alpha$  secreted into culture supernatants was significantly increased ( $p < 0.001$ ) (Figure 5a). However, pre-treatment with artemether (10, 20 and 40  $\mu\text{M}$ ) resulted in a significant and concentration-dependent reduction of TNF $\alpha$  production relative to the LPS control (~1.6-fold,  $p < 0.01$  at 10  $\mu\text{M}$ ; ~3-fold,  $p < 0.001$  at 20  $\mu\text{M}$ ; ~8-fold,  $p < 0.001$  at 40  $\mu\text{M}$ ). We also observed that LPS stimulation resulted in elevated levels of IL-6 production, which was significantly reduced when cells were pre-treated with artemether (5-40  $\mu\text{M}$ ) (~1.6-fold,  $p < 0.01$  at 5  $\mu\text{M}$ ; ~1.9-fold,  $p < 0.01$  at 10  $\mu\text{M}$ ; ~2.5-fold,  $p < 0.001$  at 20  $\mu\text{M}$ ; ~3.7-fold,  $p < 0.001$  at 40  $\mu\text{M}$ ) (Figure 5b).

### **3.5 Artemether inhibited nuclear transactivation of NF- $\kappa$ B in BV2 microglia**

In order to determine whether artemether had any general effect on NF- $\kappa$ B mediated gene transcription, NF- $\kappa$ B luciferase reporter gene assay was conducted in BV2 cells. Results obtained showed that artemether (5-40  $\mu\text{M}$ ) produced dose-dependent inhibition of NF- $\kappa$ B regulated luciferase reporter gene expression following stimulation with LPS (1  $\mu\text{g/ml}$ ) (Figure 6a). The specific NF- $\kappa$ B inhibitor, BAY 11-7085 (10  $\mu\text{M}$ ) produced ~3-fold inhibition of NF- $\kappa$ B transactivation.

### **3.6 Artemether inhibited neuroinflammation by interfering with I $\kappa$ B/NF- $\kappa$ B signalling**

Experiments to further understand the molecular mechanisms involved in the inhibitory actions of artemether on neuroinflammation showed that the drug significantly inhibited I $\kappa$ B phosphorylation and degradation following LPS activation. Stimulation of BV2 microglia with LPS (1  $\mu\text{g/ml}$ ) resulted in marked increase in the level of phospho-I $\kappa$ B protein (Figure 6b). With 5  $\mu\text{M}$  of artemether, there was no significant effect on I $\kappa$ B phosphorylation. However, pre-treatment with artemether (10-40  $\mu\text{M}$ ) resulted in a significant reduction ( $p < 0.01$ ) in the level of phospho-I $\kappa$ B

protein, when compared with LPS control (Figure 6b). LPS also induced degradation of I $\kappa$ B, which was significantly ( $p < 0.01$ ) by 10, 20 and 40  $\mu$ M, but not 5  $\mu$ M of artemether (6c). The NF- $\kappa$ B inhibitor, BAY 11-7085 (10  $\mu$ M) inhibited LPS-induced phosphorylation and degradation of I $\kappa$ B to the same degree as artemether (40  $\mu$ M). These results suggest that artemether inhibited LPS-induced I $\kappa$ B phosphorylation at higher concentrations than 5  $\mu$ M.

Subsequently, we investigated the effect of artemether on nuclear translocation of p65NF- $\kappa$ B sub-unit. Immunofluorescence experiments (Figure 6d) showed that LPS induced localisation of NF- $\kappa$ B in the nucleus. Pre-treatment with artemether (5-40  $\mu$ M) and BAY 11-7085 (10  $\mu$ M) resulted in suppression of nuclear accumulation of NF- $\kappa$ B. Further investigations using western blot revealed that LPS stimulation of BV2 microglia resulted in a marked increase in levels of nuclear p65 subunit when compared to the unstimulated control (Figure 6d). There was no significant effect on LPS-induced nuclear translocation of NF- $\kappa$ B when cells were pre-treated with 5  $\mu$ M of artemether. However, pre-treatment with 10, 20 and 40  $\mu$ M of the drug resulted in significant suppression of nuclear translocation of p65 subunit. The degree of inhibition of nuclear translocation produced by artemether (40  $\mu$ M) was similar to BAY 11-7085 (10  $\mu$ M).

We also investigated the effect of artemether on DNA binding of NF- $\kappa$ B using an ELISA-based EMSA. Figure 6f shows that stimulation of BV2 cells with LPS (1  $\mu$ g/ml) resulted in an increase in DNA binding of NF- $\kappa$ B, when compared with unstimulated control cells. When cells were treated with artemether (5-40  $\mu$ M), there was a dose-dependent and significant attenuation of DNA binding of NF- $\kappa$ B. The pronounced effect of artemether in this experiment seems to suggest that the impact of the drug on NF- $\kappa$ B signalling is more pronounced on DNA binding.

### **3.7 Inhibition of p38 MAPK signalling contributes to the effect of artemether on activated BV2 microglia**

We investigated whether inhibition of p38 activity contributed to the anti-inflammatory effect of artemether and found that stimulation of BV2 microglia for 1 h resulted in a marked increase in the levels of phospho-p38 protein when compared to the untreated control (Figure 7a). However, pre-treatment with artemether resulted in a

significant reduction in the level of phospho-p38 (~0.5-fold,  $p < 0.05$  at 5  $\mu\text{M}$ ; ~1.2-fold,  $p < 0.01$  at 10  $\mu\text{M}$ ; ~1.4-fold,  $p < 0.001$  at 20  $\mu\text{M}$ ; ~1.6-fold,  $p < 0.001$  at 40  $\mu\text{M}$ ). Levels of phospho-p38 protein in cells pre-treated with the specific p38 inhibitor, SKF86002 (1  $\mu\text{M}$ ) were similar to levels in artemether (40  $\mu\text{M}$ )-treated cells.

To further elucidate the effect of artemether on p38 MAPK signalling, we investigated its effect on the upstream kinase, MKK3/6. Results showed elevated levels of phosphorylated MKK3/6 in LPS-stimulated BV2 cells (Figure 7 b). However, this effect was significantly reduced by pre-treatment with artemether (~1.1-fold,  $p < 0.05$  at 5  $\mu\text{M}$ ; ~1.2-fold,  $p < 0.01$  at 10  $\mu\text{M}$ ; ~1.4-fold,  $p < 0.001$  at 20  $\mu\text{M}$ ; ~1.6-fold,  $p < 0.001$  at 40  $\mu\text{M}$ ) compared to the LPS control.

We also observed elevated levels of phospho-MAPKAPK2 protein expression following stimulation of BV2 cells with LPS (Figure 7c). Pre-treatment with artemether blocked phospho-MAPKAPK2 protein expression (~1.1-fold,  $p < 0.05$  at 5  $\mu\text{M}$ ; ~1.1-fold,  $p < 0.05$  at 10  $\mu\text{M}$ ; ~1.4-fold,  $p < 0.001$  at 20  $\mu\text{M}$ ; ~1.7-fold,  $p < 0.001$  at 40  $\mu\text{M}$ ) (Figure 7 c).

### **3.8 Artemether inhibited LPS-induced A $\beta$ and BACE-1 production**

To investigate the effects of artemether on levels of amyloid-related proteins, we tested the effect of the drug on A $\beta$  production following stimulation with LPS (1  $\mu\text{g/ml}$ ). Figure 8a shows that stimulation with LPS resulted in a marked increase in A $\beta$  production when compared to the untreated control. Pre-treatment with artemether (10-40  $\mu\text{M}$ ) resulted in a concentration-dependent and significant ( $p < 0.01$ ) reduction in A $\beta$  production relative to the LPS control.

Subsequent investigation of BACE-1 protein showed that stimulation of BV2 cells with LPS (1  $\mu\text{g/ml}$ ) resulted in a significant increase in the production of BACE-1. Pre-treatment with artemether (10-40  $\mu\text{M}$ ) caused a significant ( $p < 0.05$ ) reduction in BACE-1 production (Figure 8b).

### **3.9 Artemether activated Nrf2 antioxidant protective mechanisms in BV2 microglia**

We explored whether the Nrf2 antioxidant pathway played any role in the anti-neuroinflammatory actions of artemether. First, the effect of artemether on the levels of HO-1 protein was investigated in BV2 microglia. Results from these experiments

showed that in comparison with untreated cells, levels of HO-1 was increased 3-fold 24 hours after treatment with 40  $\mu\text{M}$  artemether (Figure 9a). Next we investigated the effects of artemether on NQO1 protein expression in BV2 microglia. Interestingly, artemether (5-40  $\mu\text{M}$ ) produced a significant ( $p < 0.001$ ) and dose-dependent increase in the levels of NQO1 protein (Figure 9b). We also used a luminescence-based glutathione assay to demonstrate a dose-dependent increase in the levels of GSH in BV2 microglia by 5, 10, 20 and 40  $\mu\text{M}$  artemether (Figure 9c).

Encouraged by the outcome of experiments on the effects of artemether on protein levels of Nrf2-regulated antioxidant genes, we next tested whether the effects of the drug were mediated through activation of the antioxidant responsive elements by using a luciferase reporter which is under the control of a promoter containing the ARE consensus. Using this reporter assay, we observed that artemether produced a dose-dependent increase in ARE luciferase activity in BV2 microglia (Figure 9d)

Based on this observation, we carried out experiments to determine whether artemether could enhance nuclear translocation of Nrf2. Using western blot, we were able to demonstrate that treatment of BV2 microglia with artemether (5-40  $\mu\text{M}$ ) resulted in a significant and dose-dependent increase in accumulation of Nrf2 protein in the nucleus (Figure 9e). This observation was further confirmed with results from immunofluorescence experiments (Figure 9f). Using an EMSA for Nrf2 which employs immobilised oligonucleotide containing the ARE binding site 5' GTCACAGTGA CT CAGCAGAATCTG-3', we also showed that artemether (5-40  $\mu\text{M}$ ) produced a dose-related increase in DNA binding of Nrf2 (Figure 9g).

### **3.10 Artemether prevented neuroinflammation-mediated neurotoxicity in HT22 cells**

Encouraged by the observation that artemether could block LPS-induced neuroinflammation in LPS-activated microglia, we went further to investigate whether the drug could prevent neuroinflammation-mediated neuronal death in a BV2 microglia/HT22 neuron co-culture. Following stimulation of BV2 microglia with LPS (1  $\mu\text{g/ml}$ ), there was a marked reduction in the viability of co-cultured HT22 cells (Figure 10a). Pre-treatment of BV2 microglia with artemether (10-40  $\mu\text{M}$ ) significantly ( $p < 0.05$ ) prevented toxicity to HT22 cells, as a result of stimulating BV2 microglia with LPS.

Further experiments on DNA fragmentation showed that LPS-stimulation of BV2 cells significantly increased DNA fragmentation in HT22 cells (Figure 10b). Treatment of BV2 cells with artemether prior to LPS stimulation resulted in a significantly ( $p < 0.05$ ) reduction in HT22 DNA fragmentation. We also found that stimulation of BV2 cells with LPS (1  $\mu\text{g/ml}$ ) significantly ( $p < 0.001$ ) increased intracellular ROS production in HT22 neurons (Figure 10c). Generation of cellular ROS was inhibited in a concentration-dependent manner with 5 and 10  $\mu\text{M}$  of artemether. However, as the concentration of the drug was increased to 20 and 40  $\mu\text{M}$ , a significant inhibition of ROS generation was still observed, but the potency of the drug diminished.

### **3.11 Anti-neuroinflammatory activity of artemether is dependent on Nrf2 activity in LPS-activated BV2 microglia.**

Encouraged by the outcome of our experiments on the effects of artemether on Nrf2, we next wanted to determine whether anti-inflammatory effect of the drug was dependent on Nrf2 activity. To achieve this, control siRNA- and Nrf2 siRNA-transfected BV2 cells were pre-treated with artemether (40  $\mu\text{M}$ ) and stimulated with LPS for 24 h. Western blot experiments to determine transfection efficiency showed that BV2 microglia transfected with control siRNA expressed nuclear Nrf2 protein. However, following transfection of BV2 microglia with Nrf2 siRNA, there was a marked reduction in the levels of nuclear Nrf2 in the cells (Figure 11a). Figure 11b shows that artemether (40  $\mu\text{M}$ ) produced significant reduction in LPS-induced  $\text{PGE}_2$  production in control siRNA transfected cells. In Nrf2 siRNA transfected cells however, the suppressive effects of the same concentration of artemether was significantly reversed. Similar trends were observed in experiments to determine the effects of Nrf2 knockout on the inhibition of  $\text{TNF}\alpha$  (Figure 11c) and IL-6 (Figure 11d) production, as well as NF- $\kappa\text{B}$ -DNA binding (Figure 11e) by artemether (40  $\mu\text{M}$ ).

### **3.12 Neuroprotective effects of artemether is dependent on Nrf2 activity**

Having shown that Nrf2 is required for the anti-inflammatory effect of artemether, we also sought to know if this transcription factor was needed for the neuroprotective activity of the drug in a BV2 microglia-HT22 neuron co-culture. Control siRNA- and Nrf2 siRNA-transfected microglia were co-cultured with HT22 mouse hippocampal neurons. BV2 microglia were then stimulated with LPS (1  $\mu\text{g/ml}$ ), as described

earlier. Figure 12a shows that pre-treatment of BV2 microglia with artemether (40  $\mu$ M) prior to LPS stimulation of control siRNA-transfected cells resulted in protection of HT22 neurons from toxicity. In Nrf2 siRNA-transfected cells, the neuroprotective effect of artemether was significantly lost, in comparison with control siRNA-transfected cells.

Results obtained from DNA fragmentation experiments showed that DNA fragmentation was increased in HT22 cells co-cultured with Nrf2 knockout BV2 microglia pre-treated with artemether (40  $\mu$ M) prior to LPS stimulation compared with neurons co-cultured with control siRNA-transfected BV2 microglia (Figure 12b). This suggests that the inhibitory effect of artemether on neuroinflammation-induced DNA fragmentation in the neurons was reversed following Nrf2 knockout in BV2 microglia.

#### **4. Discussion**

Microglial activation is known to play a crucial role in neuroinflammation through excessive production of pro-inflammatory mediators. Microglial-mediated inflammation has also been linked to the pathogenesis of CNS diseases [22]. Consequently, we have investigated the anti-neuroinflammatory property of artemether in LPS-activated BV2 cells.

Activated microglia produce various pro-inflammatory mediators including prostaglandins, cytokines, reactive oxygen species, and reactive nitrogen species such as nitric oxide (NO), all of which promote neuronal damage [23]. We have shown that artemether reduced the production of nitric oxide, PGE<sub>2</sub>, TNF $\alpha$  and IL-6 in LPS-activated BV2 microglia. Earlier studies in rats showed that artemether reduced collagen-induced paw oedema and nitric oxide formation [20]. This would be the first attempt at elucidating the possible mechanisms involved in the anti-inflammatory property of artemether as reported by Cuzzocrea et al. Further experiments showed that artemether reduced the levels of iNOS protein, demonstrating that the effect of the drug on NO production was due to its ability to inhibit iNOS protein. Coupled with epidemiological studies linking COX-2 inhibition to moderation in the onset of diseases like AD, several reports have suggested that mPGES-1 could be a strategy in treating this condition. For example, A $\beta$  has been shown to induce mPGES-1 expression in rat astrocytes and mouse cerebral neuronal cells [24]. In this study, we have also shown for the first time that

artemether reduced the levels of both COX-2 and mPGES-1 protein in LPS-activated microglia. The outcome showing that this drug targets both enzymes that act sequentially in the biosynthesis of PGE<sub>2</sub> during inflammation suggests that it might be acting on a central factor which regulates the genes encoding both proteins.

The NF- $\kappa$ B signalling pathway is known to regulate the genes involved in the production of pro-inflammatory mediators including the pro-inflammatory cytokines, iNOS, COX-2 and mPGES-1. Pharmacological inhibition of this transcription factor has been shown to block the production of these mediators [25-27]. In this study, artemether has been shown to attenuate the production of NO/iNOS, PGE<sub>2</sub>/COX-2/mPGES-1, as well as the pro-inflammatory cytokines TNF $\alpha$  and IL-6. We therefore explored its effect on NF- $\kappa$ B activity. Reporter gene assays on LPS-stimulated BV2 microglia transfected with an NF- $\kappa$ B vector showed that artemether inhibited NF- $\kappa$ B-driven luciferase expression, suggesting that the drug might possess inhibitory actions against the NF- $\kappa$ B signalling pathway. We further demonstrated that artemether suppressed phosphorylation and degradation of I $\kappa$ B. The highest concentration of artemether used in our investigation (40  $\mu$ M) produced affected I $\kappa$ B to the same degree as BAY 11-7085, a specific inhibitor of NF- $\kappa$ B. Artemether also inhibited nuclear translocation and DNA binding of NF- $\kappa$ B in LPS-activated BV2 microglia. These results suggest that artemether targets NF- $\kappa$ B signalling in activated microglia through mechanisms involving upstream targets resulting in nuclear translocation, as well as DNA binding of NF- $\kappa$ B. We have shown earlier that a water-soluble semi-synthetic derivative of artemisinin, artesunate inhibited I $\kappa$ B phosphorylation and degradation as well as nuclear p65 translocation to the nucleus following stimulation of BV2 microglia with LPS/IFN $\gamma$  [26]. Studies by Zhu et al. (2012) also showed that artemisinin inhibited I $\kappa$ B phosphorylation and p65 NF- $\kappa$ B translocation to the nucleus in LPS activated primary microglia cells [28]. It therefore appears that artemisinin derivatives, including artemether might be inhibiting LPS-induced neuroinflammation by targeting similar mechanisms involving the NF- $\kappa$ B signalling pathway.

Mitogen-activated protein kinases are intracellular enzymes that allow cells to respond to stimuli from the extracellular environment [29]. The p38MAPK signalling has been shown to be critical in the expression and activity of pro-inflammatory

cytokines in the CNS [30]. In addition, p38 is involved in regulating the production of crucial inflammatory mediators such as COX-2 in macrophages [31]. Furthermore, studies have shown that pharmacological inhibition of p38 $\alpha$  MAPK in an AD mouse model decreases brain pro-inflammatory cytokine production and attenuates synaptic protein loss [29]. Studies also showed that the deficiency of microglial p38 $\alpha$  MAPK rescued neurons and reduces synaptic protein loss by suppressing LPS-induced TNF $\alpha$  production [30]. Consequently, pharmacological modulation of p38MAPK signalling following LPS stimulation of the microglia is an important strategy in preventing neurodegeneration. We showed that artemether produced negative modulation of p38 signalling pathway following stimulation of BV2 microglia, through inhibition of phosphorylation of p38 and its upstream kinase MKK3/6. At a concentration of 40  $\mu$ M, the degree of inhibition was similar to that produced by SKF86002 (1  $\mu$ M). We also showed that artemether inhibited MAPKAPK2, the kinase which acts on p38. These results suggest that the anti-inflammatory action of artemether in LPS-activated microglia is mediated in part through the interference of p38 MAPK signalling pathway.

Neuroinflammation is associated with the generation of A $\beta$  in the brains of AD patients [32]. Furthermore, NF- $\kappa$ B controls the expression of BACE-1 and thus A $\beta$  formation [33]. In addition, studies have shown that amyloid- $\beta$  and BACE-1 were detected in microglia following LPS stimulation [34]. Previous studies have reported that AD brains contain increased levels of BACE-1 and NF- $\kappa$ B p65, and that NF- $\kappa$ B p65 expression leads to an increase in BACE-1 promoter activity and BACE-1 transcription [35]. Artemether decreased the production of A $\beta$  and BACE-1 following LPS stimulation, suggesting that the ability of the drug to suppress these proteins of amyloidogenesis was closely linked to its anti-neuroinflammatory effect.

The antioxidant transcription factor, Nrf2 which binds to the antioxidant response element (ARE) in gene promoters is known to regulate various endogenous cytoprotective genes, including those encoding for anti-inflammatory proteins. Nrf2 activity has been reported to be crucial in the down-regulation of neuroinflammation [36]. Several studies have suggested that Nrf2 may have a modulatory effect on activation of NF- $\kappa$ B during neuroinflammation. Also, compounds which inhibit NF- $\kappa$ B activation have been shown to activate Nrf2. For instance, we have reported that tiliroside, a compound which inhibited NF- $\kappa$ B in BV2 microglia, also activated Nrf2

[27]. In addition, Foresti et al. (2013) showed that small molecule activators of the Nrf2-HO-1 antioxidant axis modulate inflammation in BV2 microglia cells [37]. Consequently, we were interested to know if artemether also had a similar effect in BV2 microglia. Firstly, we demonstrated that artemether increased levels of HO-1, a protein that has been shown to increase cellular resistance to inflammation [38]. This observation seems to suggest that artemether could be suppressing neuroinflammation through mechanisms that increase levels of HO-1 in the microglia. We also showed that artemether increased levels of antioxidant protein, NQO1, as well as endogenous levels of GSH.

Encouraged by the effects of artemether on antioxidant proteins, we proceeded to fully understand whether Nrf2 played any roles in the observed effects. Our first efforts showed that the activity of the antioxidant responsive element was increased by artemether, suggesting that the drug enhanced ARE-promoter dependent transcription. On activation, Nrf2 is translocated to the nucleus where it binds to ARE to induce the expression of ARE-dependent genes [39]. We therefore thought that the next step in our investigation was to determine the effects of artemether on nuclear translocation of Nrf2. Artemether increased nuclear translocation of Nrf2, as well as its binding to ARE in the microglia. Taken together, our results show that artemether enhances the transcriptional activity of Nrf2 in BV2 microglia. Artesunate, which is related drug to artemether has been reported to activate Nrf2 in BV2 microglia [40], and in mice lungs [41, 42]. It would therefore be interesting to elucidate the relationship between the chemical nature of these drugs and their effects on Nrf2 signalling.

Chronic neuroinflammation results in the production of pro-inflammatory mediators including cytokines which are neurotoxic to adjacent neurons [43]. In theory, drugs which inhibit neuroinflammation and hence the production of neurotoxic mediators would be expected to exhibit some neuroprotective effects. The most effective approach to test the neuroprotective effect of an anti-inflammatory drug is to use a neuron-microglia co-culture, which provides a system for both cells to be grown in close proximity. Using this approach, we cultured BV2 microglia in a transwell system that was placed above an HT22 neuronal layer. Using this model, we showed that stimulating BV2 microglia with LPS resulted in reduced viability of HT22 hippocampal neurons. Treatment with artemether prior to stimulation of BV2

microglia however prevented death of adjacent HT22 in the co-culture, an outcome that might suggest that artemether prevented neurotoxicity due to its anti-inflammatory effect in the microglia. These observations were further confirmed in experiments showing that artemether prevented inflammation-induced DNA fragmentation in HT22 cells. Results obtained from experiments on the production of ROS by HT22 following LPS activation of co-cultured BV2 microglia was however different. While the effects of artemether on HT22 neuron viability and DNA fragmentation were dose-dependent, we observed that pre-treatment with the drug reduced ROS production by HT22 neurons in a dose-related fashion up to 10  $\mu\text{M}$ . However, as the concentration was increased to 20 and 40  $\mu\text{M}$ , the ROS suppressive effect of the drug was reduced. There have been suggestions in scientific literature that artemisinin-related drugs have an endoperoxide bridge whose cleavage results in the generation of ROS in cancer cells [44]. While there is no evidence about the direct effects of artemether on ROS generation in neurons, we propose that the ability of the drug to reduce inflammation-induced ROS in neurons is reduced at high concentrations, possibly due to the increased influence of the endoperoxide bridge.

Our studies have shown that artemether inhibits neuroinflammation and activates Nrf2 in BV2 microglia. Consequently, we were interested in establishing a direct link between the two activities of the drug. We compared the effects of the drug in BV2 microglia transfected with control siRNA (non-targeting siRNA) and cells transfected with mouse Nrf2 siRNA. Western blot analysis showed that Nrf2 gene was successfully knocked down in these experiments. BV2 microglia transfected with control siRNA expressed Nrf2 protein, while there was a clear downregulation of the protein in the knockout cells.

Our results showed that artemether reduced the production of pro-inflammatory cytokines (TNF $\alpha$  and IL-6), and PGE $_2$  in control siRNA-transfected cells. However, Nrf2 knockout reversed the observed inhibitory effects of artemether on the production of inflammatory mediators in LPS-activated microglia. To our knowledge, this was the first report linking the anti-inflammatory property of artemether in LPS-activated microglia to Nrf2 activity. Similar to results obtained in BV2 microglia monoculture, we showed that knockout of Nrf2 in the BV2 microglia resulted in the loss of protective effect by artemether in HT22 cells in a co-culture. This further

confirmed that artemether produces neuroprotective effect by inhibiting neuroinflammation.

We conclude that artemether inhibits neuroinflammation as well as the resulting amyloidogenesis and neurotoxicity. It is suggested that the drug acts through multiple targets involving both NF- $\kappa$ B and p38 MAPK signalling. The study further established that the effects of artemether are dependent on Nrf2 antioxidant protective mechanisms suggesting that the drug might be a potential therapeutic strategy in neurodegenerative conditions like AD.

**Conflict of Interest:** The authors declare that they have no conflict of interest.

Accepted Manuscript

List of Abbreviations:

AA	Arachidonic acid
AD	Alzheimer's disease
ANOVA	Analysis of variance
BACE-1	beta-site amyloid precursor protein cleaving enzyme 1
CNS	Central Nervous System
COX	Cyclooxygenase
DMSO	Dimethyl sulphoxide
FBS	Foetal bovine serum
HEK 293	Human Embryonic Kidney 293
I $\kappa$ B	Inhibitor of Kappa B
IKK	I $\kappa$ B kinase
IL	Interleukin
iNOS	Inducible nitric oxide synthase
LPS	Lipopolysaccharide
MAPK	Mitogen-activated protein kinase
HO-1	Heme oxygenase-1
NO	Nitric oxide
Nrf2	Nuclear factor-erythroid 2-related factor 2
NF- $\kappa$ B	Nuclear Factor kappa B
TNF- $\alpha$	Tumour necrosis factor-alpha

## **Acknowledgements**

Uchechukwu P Okorji and Ravikanth Velagapudi are funded by a partial PhD scholarship from the University of Huddersfield. Abdelmeneim El-Bakoush was funded by a PhD scholarship from the Libyan Government. This study was partially funded by the University of Huddersfield (University Research Fund/International Networking Fund) awarded to Dr Olumayokun Olajide.

Accepted Manuscript

## References

1. Salter M, Beggs S (2014) Sublime microglia: Expanding roles for the guardians of the CNS. *Cell* 158 (1): 15-24.
2. Perry V, Teeling J (2013) Microglia and macrophages of the central nervous system: the contribution of microglia priming and systemic inflammation to chronic neurodegeneration. *Semin Immunopathol* 35 (5): 601-612.
3. Mosher K, Wyss-Coray T (2014) Microglial dysfunction in brain aging and Alzheimer's disease. *Biochem Pharmacol* 88 (4): 594-604.
4. Prokop S, Miller KR, Heppner FL (2013) Microglia actions in Alzheimer's disease. *Acta Neuropathol* 126 (4): 461-477.
5. Kaltschmidt B, Kaltschmidt C (2009) NF-kappaB in the nervous system. *Cold Spring Harb Perspect Biol.* 1(3):a001271. doi: 10.1101/cshperspect.a001271.
6. Yong H, Koh M, Moon A (2009) The p38MAPK inhibitors for the treatment of inflammatory diseases and cancer. *Expert Opin Investig Drugs* 18 (12): 1893-1905.
7. Corrêa S, Eales K (2012) The role of p38 MAPK and Its substrates in neuronal plasticity and neurodegenerative disease. *J Signal Transduct.* 2012:649079. doi: 10.1155/2012/649079.
8. Kremontsov DN, Thornton TM, Teuscher C, Rincon M (2013) The emerging role of p38 mitogen-activated protein kinase in multiple sclerosis and its models. *Mol Cell Biol.* 33 (19): 3728-3734.
9. Diego G, Hugh P (2015) Microglial dynamics and role in the healthy and diseased brain: A paradigm of functional plasticity. *Neuroscientist* 21(2):169-184.
10. Wu LH, Lin C, Lin HY, Liu YS, Wu CY, Tsai CF, Chang PC, Yeh WL, Lu DY (2015) Naringenin suppresses neuroinflammatory responses through inducing suppressor of cytokine signaling 3 expression. *Mol Neurobiol.* doi:10.1007/s12035-014-9042-9
11. Heneka M, O'Banion M (2007) Inflammatory processes in Alzheimer's disease. *J Neuroimmunol.* 184 (1-2): 69-91.
12. Lee JW, Lee YK, Yuk DY, Choi DY, Ban SB, Oh KW, Hong JT (2008) Neuroinflammation induced by lipopolysaccharide causes impairment through

- enhancement of beta-amyloid generation. *J Neuroinflammation* 5:37. doi: 10.1186/1742-2094-5-37.
13. Lee YJ, Choi DY, Choi IS, Han JY, Jeong HS, Han SB, Oh KW, Hong JT (2011) Inhibitory effect of a tyrosine-fructose Maillard reaction product, 2,4-bis(p-hydroxyphenyl)-2-butenal on amyloid- $\beta$  generation and inflammatory reactions via inhibition of NF- $\kappa$ B and STAT3 activation in cultured astrocytes and microglial BV-2 cells. *J Neuroinflammation* 8:132. doi: 10.1186/1742-2094-8-132.
  14. Song SY, Jung YY, Hwang CJ, Lee HP, Sok CH, Kim JH, Lee SM, Seo HO, Hyun BK, Choi DY, Han SB, Ham YW, Hwang BY, Hong JT (2014) Inhibitory effect of ent-Sauchinone on amyloidogenesis via inhibition of STAT3-mediated NF- $\kappa$ B activation in cultured astrocytes and microglial BV-2 cells. *J Neuroinflammation* 11:118. doi: 10.1186/1742-2094-11-118.
  15. Rojo AI, McBean G, Cindric M, Egea J, López MG, Rada P, Zarkovic N, Cuadrado A (2014) Redox control of microglial function: Molecular mechanisms and functional significance. *Antioxid Redox Signal*. 21(13): 1766-1801.
  16. Kapturczak MH, Wasserfall C, Brusko T, Campbell-Thompson M, Ellis TM, Atkinson MA, Agarwal A (2004) Heme oxygenase-1 modulates early inflammatory responses: evidence from the heme oxygenase-1-deficient mouse. *Am J Pathol*. 165(3): 1045-1053.
  17. Kanninen K, Malm TM, Jyrkkänen HK, Goldsteins G, Keksa-Goldsteine V, Tanila H, Yamamoto M, Ylä-Herttuala S, Levonen AL, Koistinaho J (2008) Nuclear factor erythroid 2-related factor 2 protects against beta amyloid. *Mol Cell Neurosci* 39 (3): 302-313.
  18. Ramsey CP, Glass CA, Montgomery MB, Lindl KA, Ritson GP, Chia LA, Hamilton RL, Chu CT, Jordan-Sciutto KL (2007) Expression of Nrf2 in neurodegenerative diseases. *J Neuropathol Exp Neurol* 66(1): 75-85.
  19. Miller LH, Su X (2011) Artemisinin: discovery from chinese herbal garden. *Cell* 146 (6): 855-858.
  20. Cuzzocrea S, Saadat F, Di Paola R, Mirshafiey A (2005) Artemether: a new therapeutic strategy in experimental rheumatoid arthritis. *Immunopharmacol Immunotoxicol* 27 (4): 615-630.

21. Wu J (2011) Investigation of anti-inflammatory effect of artemether in mouse model of colitis. *Inflamm Bowel Dis.* 17: S18-S19.
22. Zhang F, Wang H, Wu Q, Lu Y, Nie J, Xie X, Shi J (2013) Resveratrol protects cortical neurons against microglia-mediated neuroinflammation. *Phytother Res.* 27(3):344-349.
23. Gao HM, Hong JS (2008) Why neurodegenerative diseases are progressive: uncontrolled inflammation drives disease progression. *Trends Immunol* 29 (8): 57–65.
24. Kuroki Y, Sasaki Y, Kamei D, Akitake Y, Takahashi M, Uematsu S, Akira S, Nakatani Y, Kudo I, Hara S (2012) Deletion of microsomal prostaglandin E synthase-1 protects neuronal cells from cytotoxic effects of  $\beta$ -amyloid peptide fragment 31–35. *Biochem Biophys Res Commun* 424 (3): 409–413.
25. Olajide OA, Kumar A, Velagapudi R, Okorji UP, Fiebich BL (2014) Punicalagin inhibits neuroinflammation in LPS-activated rat primary microglia. *Mol. Nutr. Food Res.* 58 (9):1843-1851.
26. Okorji U, Olajide O (2014) A semi-synthetic derivative of artemisinin, artesunate inhibits prostaglandin E2 production in LPS/IFN $\gamma$ -activated BV2 microglia. *Bioorg Med Chem*, 22(17): 4726-4734.
27. Velagapudi R, Aderogba M, Olajide O (2014) Tiliroside, a dietary glycosidic flavonoid, inhibits TRAF-6/NF- $\kappa$ B/p38-mediated neuroinflammation in activated BV2 microglia. *Biochim Biophys Acta* 1840(12): 3311-3319.
28. Zhu C, Xiong Z, Chen X, Peng F, Hu X, Chen Y, Wang Q (2012) Artemisinin attenuates lipopolysaccharide-stimulated proinflammatory responses by inhibiting NF- $\kappa$ B pathway in microglia cells. *PLoS One* 7(4):e35125. doi: 10.1371/journal.pone.0035125.
29. Munoz L, Ammit A (2010) Targeting p38 MAPK pathway for the treatment of Alzheimer's disease. *Neuropharmacology* 2010. 58 (3) 561-568.
30. Xing B, Bachstetter AD, Van Eldik LJ (2011) Microglial p38 $\alpha$  MAPK is critical for LPS-induced neuron degeneration, through a mechanism involving TNF $\alpha$ . *Mol Neurodegener* 6:84. doi: 10.1186/1750-1326-6-84.
31. Hsu MJ, Chang CK, Chen MC, Chen BC, Ma HP, Hong CY, Lin CH. Apoptosis signal-regulating kinase 1 in peptidoglycan induced COX-2 expression in macrophages. *J Leukoc Biol.* 87(6):1069-1082.

32. Borchelt DR, Ratovitski T, van Lare J, Lee MK, Gonzales V, Jenkins NA, Copeland NG, Price DL, Sisodia SS (1997) Accelerated amyloid deposition in the brains of transgenic mice coexpression mutant presenilin 1 and amyloid precursor proteins. *Neuron*. 19(4):939-945.
33. Sambamurti K, Kinsey R, Maloney B, Ge YW, Lahiri DK (2004) Gene structure and organisation of human beta-secretase (BACE) promoter. *FASEB J* 18(9):1034-1036.
34. Kim JA, Yun HM, Jin P, Lee HP, Han JY, Udumula V, Moon DC, Han SB, Oh KW, Ham YW, Jung HS, Song HS, Hong JT (2014) Inhibitory effect of a 2,4-bis(4-hydroxyphenyl)-2-butenal diacetate on neuroinflammatory reactions via inhibition of STAT1 and STAT3 activation in cultured astrocytes and microglial BV-2 cells. *Neuropharmacology* 79: 476-487.
35. Chen CH, Zhou W, Liu S, Deng Y, Cai F, Tone M, Tone Y, Tong Y, Song W (2012) Increased NF- $\kappa$ B signalling up-regulated BACE-1 expression and its therapeutic potential in Alzheimer's disease. *Int J Neuropsychopharmacol*. 15 (1): 77-90.
36. Innamorato NG, Rojo AI, García-Yagüe AJ, Yamamoto M, de Ceballos ML, Cuadrado A (2008) The transcription factor Nrf2 is a therapeutic target against brain inflammation. *J Immunol*. 181 (1): 680-689.
37. Foresti R, Bains SK, Pitchumony TS, de Castro Brás LE, Drago F, Dubois-Randé JL, Bucolo C, Motterlini R (2013) Small molecule activators of the Nrf2-HO-1 antioxidant axis modulate heme metabolism and inflammation in BV2 microglia cells. *Pharmacol Res*. 76: 132-148.
38. Syapin PJ (2008) Regulation of haeme oxygenase-1 for treatment of neuroinflammation and brain disorders. *Br J Pharmacol*. 155(5):623-640.
39. Lee IS, Lim J, Gal J, Kang JC, Kim HJ, Kang BY, Choi HJ (2011) Anti-inflammatory activity of xanthohumol involves heme oxygenase-1 induction via NRF2-ARE signaling in microglial BV2 cells. *Neurochem Int*. 58(2):153-160.
40. Lee IS, Ryu DK, Lim J, Cho S, Kang BY, Choi HJ (2012) Artesunate activates Nrf2 pathway-driven anti-inflammatory potential through ERK signaling in microglial BV2 cells. *Neurosci Lett*. 509(1):17-21.

41. Ho WE, Cheng C, Peh HY, Xu F, Tannenbaum SR, Ong CN, Wong WS (2012) Anti-malarial drug artesunate ameliorates oxidative lung damage in experimental allergic asthma. *Free Radic Biol Med.* 53(3):498-507.
42. Ng DS, Liao W, Tan WS, Chan TK, Loh XY, Wong WS (2014) Anti-malarial drug artesunate protects against cigarette smoke-induced lung injury in mice. *Phytomedicine.* 21(12):1638-1644.
43. Olmos G, Lladó J (2014) Tumor necrosis factor alpha: a link between neuroinflammation and excitotoxicity. *Mediators Inflamm.* 2014:861231. doi: 10.1155/2014/861231.
44. Efferth T, Oesch F (2004) Oxidative stress response of tumor cells: microarray-based comparison between artemisinin and anthracyclines. *Biochem Pharmacol.* 68(1): 3-10.

Accepted Manuscript

## Figure Legends

**Figure 1:** Chemical structure of artemether

**Figure 2:** Artemether did not affect the viability of BV2 cells. BV2 cells were pre-treated with artemether (5-40  $\mu$ M) for 30 min and subsequently stimulated with LPS (1  $\mu$ g/ml) for 24 h. Thereafter, MTT viability assay was performed. All values are expressed as mean  $\pm$  SEM for at least 3 independent experiments. Data were analysed using one-way ANOVA for multiple comparisons with post-hoc Student Newman-Keuls test.

**Figure 3:** Artemether suppressed iNOS-mediated NO production in LPS-activated BV2 cells. Cells were stimulated with LPS (1  $\mu$ g/ml) in the presence or absence of artemether (5-40  $\mu$ M) for 24 h. Subsequently, culture supernatants and cell lysates were collected and analysed. (a) Artemether reduced NO production in LPS-activated BV2 cells. (b) Artemether inhibited levels of iNOS protein in LPS-activated BV2 cells. Cell lysates were analysed for iNOS protein using western blot. All values are expressed as mean  $\pm$  SEM for three independent experiments. Data were analysed using one-way ANOVA for multiple comparison with post hoc Student Newman-Keuls test. \* $p < 0.05$ , \*\*\* $p < 0.001$  in comparison with LPS control.

**Figure 4:** Artemether reduced PGE<sub>2</sub> production (a) through suppression of COX-2 (b) and mPGES-1 (c) expression in LPS-activated BV2 microglia cells. BV2 cells were pre-treated with artemether (5-40  $\mu$ M) and stimulated with LPS (1  $\mu$ g/ml) for 24 h. PGE<sub>2</sub> was measured in cell supernatants using PGE<sub>2</sub> EIA. COX-2 and mPGES-1 protein levels were determined with western blot. All values are expressed as mean  $\pm$  SEM for three independent experiments. Data were analysed using one-way ANOVA for multiple comparison with post hoc Student Newman-Keuls test. \*\*\* $p < 0.001$  in comparison with LPS control.

**Figure 5:** Artemether inhibited the production of pro-inflammatory cytokines in LPS-activated BV2 microglia cells. BV2 cells were stimulated with LPS (1  $\mu$ g/ml) in the presence or absence of artemether (5-40  $\mu$ M) for 24 h. Culture supernatants were collected and analysed for cytokine production using ELISA. All values are expressed as mean  $\pm$  SEM for three independent experiments. Data were analysed using one-way ANOVA for multiple comparison with post hoc Student Newman-Keuls test. \*\* $p < 0.01$ , \*\*\* $p < 0.001$  in comparison with LPS control.

**Figure 6:** Artemether inhibited neuroinflammation by targeting I $\kappa$ B/NF- $\kappa$ B signalling in LPS-activated BV2 microglia. (a) Artemether suppressed NF- $\kappa$ B luciferase activity in BV2 cells transfected with pGL4.32[luc2P/NF- $\kappa$ B-RE/Hygro] vector and stimulated with LPS (1  $\mu$ g/ml) in the absence or presence of artemether (5-40  $\mu$ M) for 6 h. (b and c) I $\kappa$ B $\alpha$  phosphorylation and degradation in LPS-activated microglia was suppressed by artemether. Protein levels of phospho- and total I $\kappa$ B was measured with western blot, using rabbit anti-phospho-I $\kappa$ B and rabbit total I $\kappa$ B antibody. (d) Artemether suppressed p65 translocation in LPS-activated BV2 microglial cells. BV2 cells were treated with artemether (5-40  $\mu$ M) prior to LPS (1  $\mu$ g/ml) for 1 h. Immunofluorescence experiments were carried out to detect p65 protein localisation using an anti-p65 antibody and Alexa Fluor 488-conjugated donkey anti-rabbit IgG antibodies. Cells were counterstained with DAPI and fluorescence images acquired with an EVOS<sup>®</sup> FLoid<sup>®</sup> cell imaging station (scale bar: 100  $\mu$ m). (e) Western blot showing inhibition of p65 translocation to the nucleus by artemether (5-40  $\mu$ M) in LPS-stimulated BV2 microglia. (f) Artemether inhibited DNA binding of NF- $\kappa$ B in LPS-stimulated BV2 microglia. Nuclear extracts from cells were added to 96-well plates to which an oligonucleotide containing the NF- $\kappa$ B consensus site (5' GGGACTTTCC-3') has been immobilised, followed by addition of NF- $\kappa$ B and HRP-conjugated antibodies. Absorbance was read in a microplate reader. All values are expressed as mean  $\pm$  SEM for at least 3 independent experiments. Data were analysed using one-way ANOVA for multiple comparisons with post-hoc Student Newman-Keuls test. \* $p$ <0.05, \*\* $p$ <0.01, \*\*\* $p$ <0.001 in comparison with LPS control.

**Figure 7:** Artemether inhibited p38MAPK-signalling pathway by reducing phospho-p38 protein (a), phospho-MKK3/6 protein (b) and phospho-MAPKAPK2 protein (c) in LPS-activated BV2 microglia cells. All values are expressed as mean  $\pm$  SEM for 3 independent experiments. All values are expressed as mean  $\pm$  SEM for at least 3 independent experiments. Data were analysed using one-way ANOVA for multiple comparisons with post-hoc Student Newman-Keuls test. \* $p$ <0.05, \*\* $p$ <0.01, \*\*\* $p$ <0.001 in comparison with LPS control.

**Figure 8:** Artemether inhibited LPS-induced A $\beta$  (a) and BACE-1 (b) levels in LPS-stimulated BV2 cells. All values are expressed as mean  $\pm$  SEM for at least 3 independent experiments. Data were analysed using one-way ANOVA for multiple

comparisons with post-hoc Student Newman-Keuls test. \* $p < 0.05$ , \*\* $p < 0.01$ , \*\*\* $p < 0.001$  in comparison with LPS control.

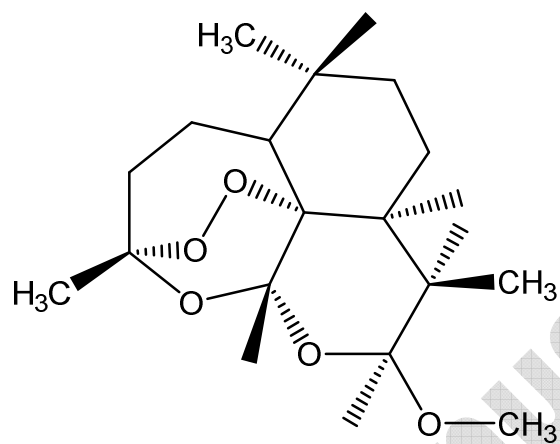
**Figure 9:** Artemether (5-40  $\mu\text{M}$ ) increased levels of HO-1 and NQO1 proteins in BV2 microglia (a, b). Cells lysates were analysed using western blots with anti-HO-1 and anti-NQO1 antibodies. (c) Artemether increases cellular levels of GSH in BV2 microglia. (d) Artemether activated ARE luciferase activity in BV2 cells transfected with pGL4.37 [luc2P/ARE/Hygro vector for 18 h. Thereafter, cells were treated with artemether (5-40  $\mu\text{M}$ ) for 8 h and luciferase activity measured. (e) Artemether (5-40  $\mu\text{M}$ ) increased levels of Nrf2 protein in BV2 microglia. Nuclear extracts analysed for Nrf2 protein using western blot with anti-Nrf2 antibody. (f) Immunofluorescence experiments were carried out to detect Nrf2 protein localisation using an anti-Nrf2 antibody and Alexa Fluor 488-conjugated donkey anti-rabbit IgG antibodies. Cells were counterstained with DAPI and fluorescence images acquired with an EVOS<sup>®</sup> FLoid<sup>®</sup> cell imaging station (scale bar: 100  $\mu\text{m}$ ). (g) Nuclear extracts from cells were added to 96-well plates to which an oligonucleotide containing the ARE consensus binding site (5' GTCACAGTGAAGTCAAGCAGAATCTG-3') has been immobilised, followed by addition of Nrf2 and HRP-conjugated antibodies. Absorbance was read in a microplate reader. All values are expressed as mean  $\pm$  SEM for at least 3 independent experiments. Data were analysed using one-way ANOVA for multiple comparisons with post-hoc Student Newman-Keuls test. \* $p < 0.05$ , \*\* $p < 0.01$ , \*\*\* $p < 0.001$  in comparison with untreated control.

**Figure 10:** Artemether produced neuroprotective effects against neuronal damage induced by LPS activation of BV2 microglia. BV2 cells were co-cultured on transwell inserts with HT22 hippocampal neurons. Microglia were stimulated with LPS (1  $\mu\text{g/ml}$ ) after treatment with artemether (5-40  $\mu\text{M}$ ). (a) MTT assay revealed an increase in HT22 viability in cells treated with artemether, in comparison with control. (b) Reduction in DNA fragmentation in HT22 cells co-cultured with LPS-stimulated BV2 microglia which were pre-treated with artemether (c) Artemether treatment caused a reduction in cellular ROS generation in HT22 cells. All values are expressed as mean  $\pm$  SEM for at least 3 independent experiments. Data were analysed using one-way ANOVA for multiple comparisons with post-hoc Student Newman-Keuls test. \* $p < 0.05$ , \*\* $p < 0.01$ , \*\*\* $p < 0.001$  in comparison with LPS control. <sup>o</sup> $p < 0.001$  in comparison with untreated control

**Figure 11:** Contribution of Nrf2 to the anti-inflammatory effect of artemether. Control siRNA- and Nrf2 siRNA-transfected BV2 cells were pre-treated with artemether (40  $\mu$ M) and stimulated with LPS for 24 h. (a) Western blot experiments on nuclear extracts shows knockout efficiency. Transfection of BV2 microglia with Nrf2 siRNA reversed suppressive effects of artemether (40  $\mu$ M) on PGE<sub>2</sub> (b), TNF $\alpha$  (c) IL-6 (d) production, NF- $\kappa$ B DNA binding (e) following LPS stimulation. All values are expressed as mean  $\pm$  SEM for at least 3 independent experiments. Data were analysed using one-way ANOVA for multiple comparisons with post-hoc Student Newman-Keuls test. \*\*p<0.01, \*\*\*p<0.001 in comparison with control siRNA-transfected cells. <sup>o</sup>p<0.001, compared with unstimulated control siRNA-transfected cells.

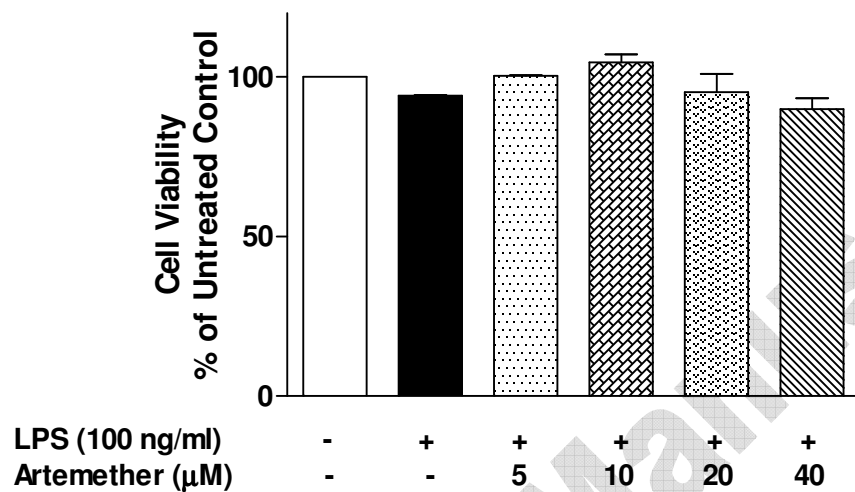
**Figure 12:** Contribution of Nrf2 to the neuroprotective effect of artemether in a BV2 microglia/HT22 hippocampal neuron co-culture. Control siRNA- and Nrf2 siRNA-transfected BV2 cells were co-cultured with HT22 neurons and pre-treated with artemether (40  $\mu$ M) followed by stimulation with LPS for 24 h. Subsequently, MTT (a) and DNA fragmentation (b) assays were carried out. All values are expressed as mean  $\pm$  SEM for at least 3 independent experiments. Data were analysed using one-way ANOVA for multiple comparisons with post-hoc Student Newman-Keuls test. \*\*p<0.01, \*\*\*p<0.001 in comparison with control siRNA-transfected cells. <sup>o</sup>p<0.001, compared with unstimulated control siRNA-transfected cells.

Figure 1



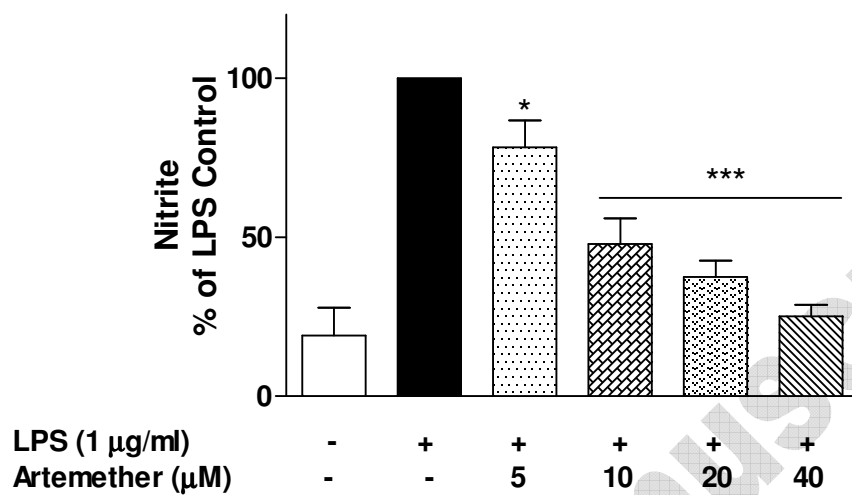
Accepted Manuscript

Figure 2



Accepted Manuscript

Figure 3a



Accepted Manuscript

Figure 3b

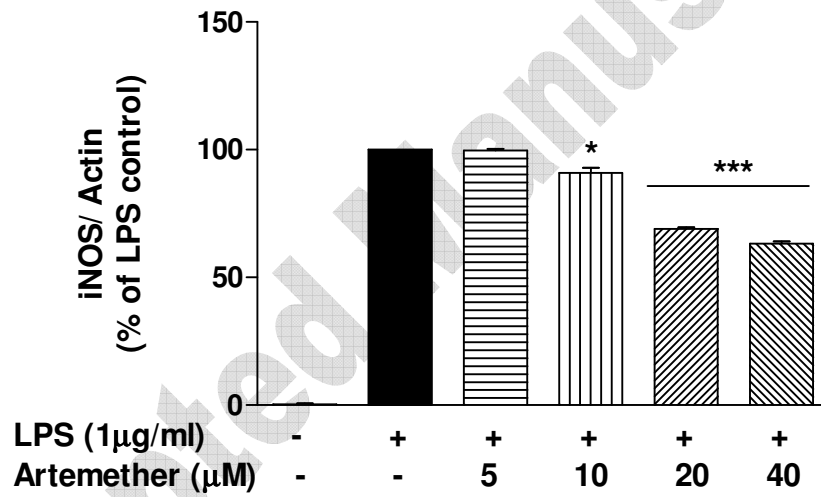
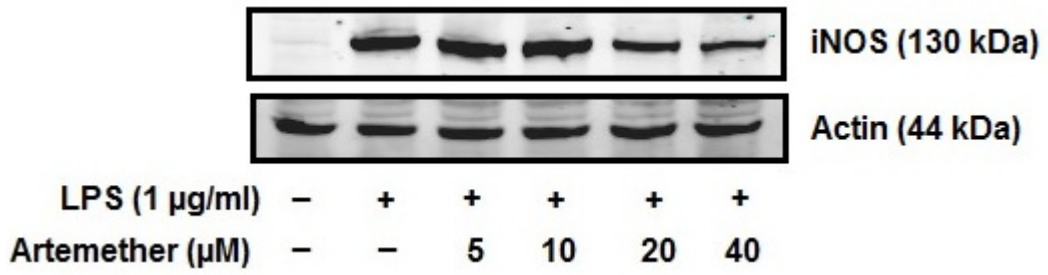
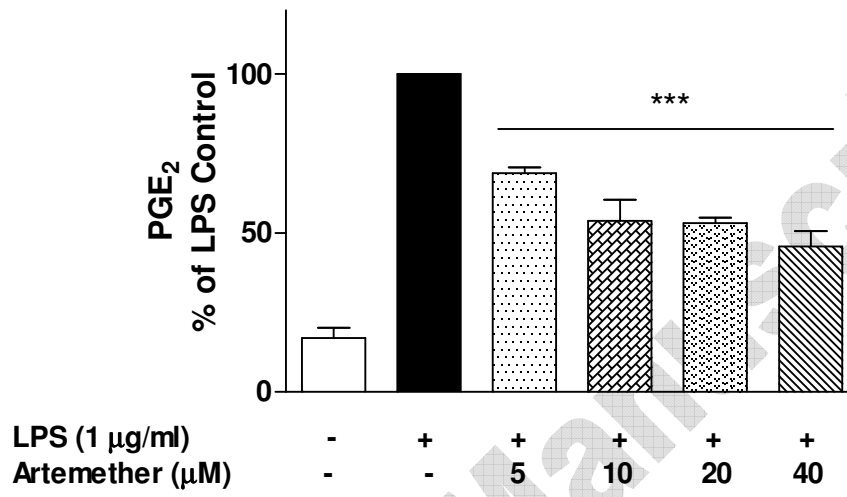


Figure 4a



Accepted Manuscript

Figure 4b

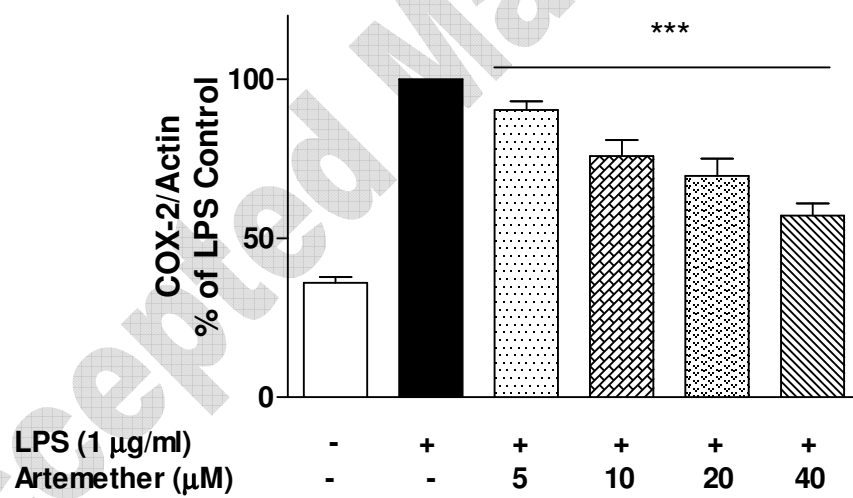
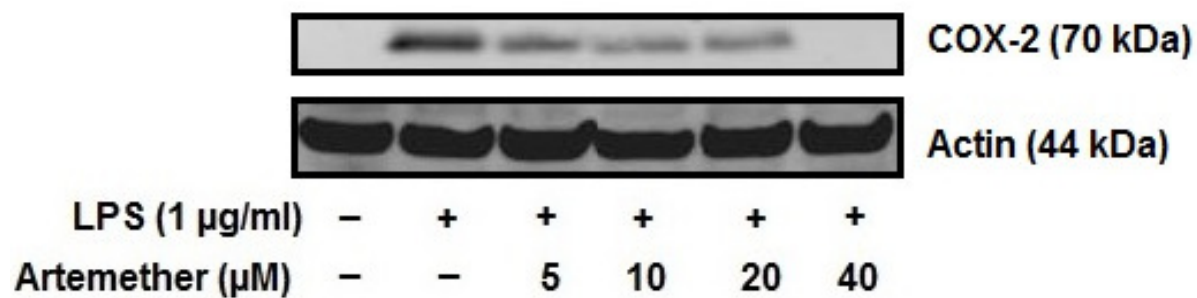


Figure 4c

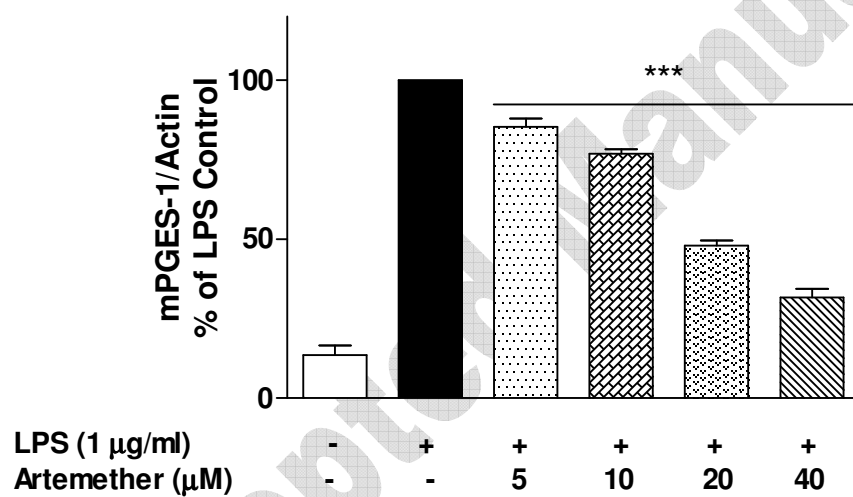
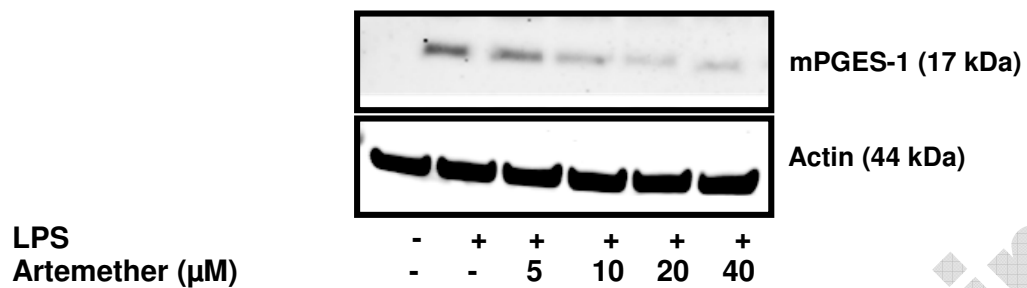
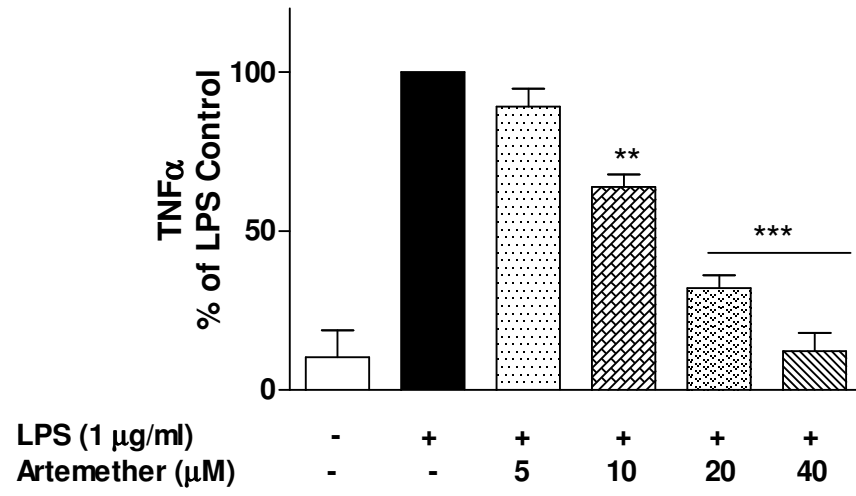
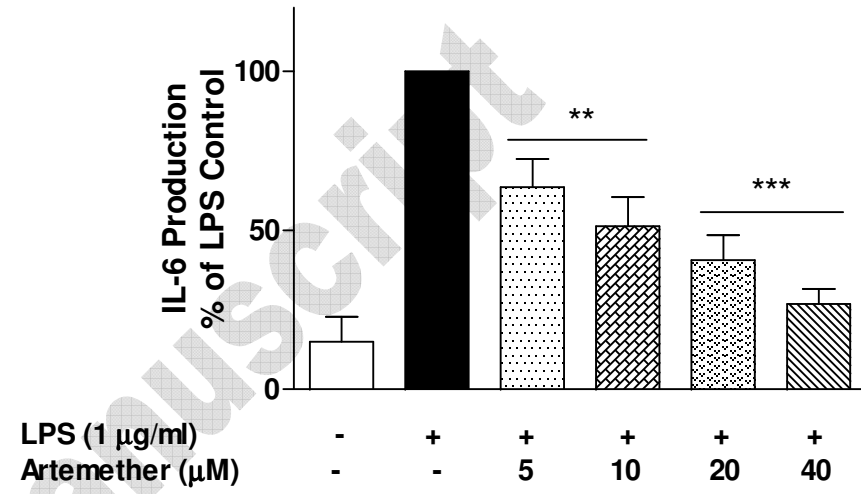


Figure 5

a

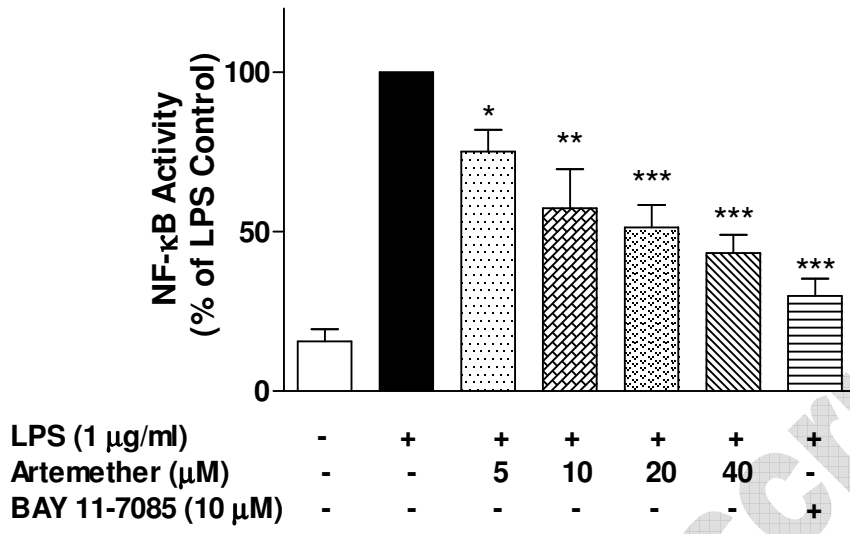


b



Accepted Manuscript

Figure 6a



Accepted Manuscript

Figure 6b

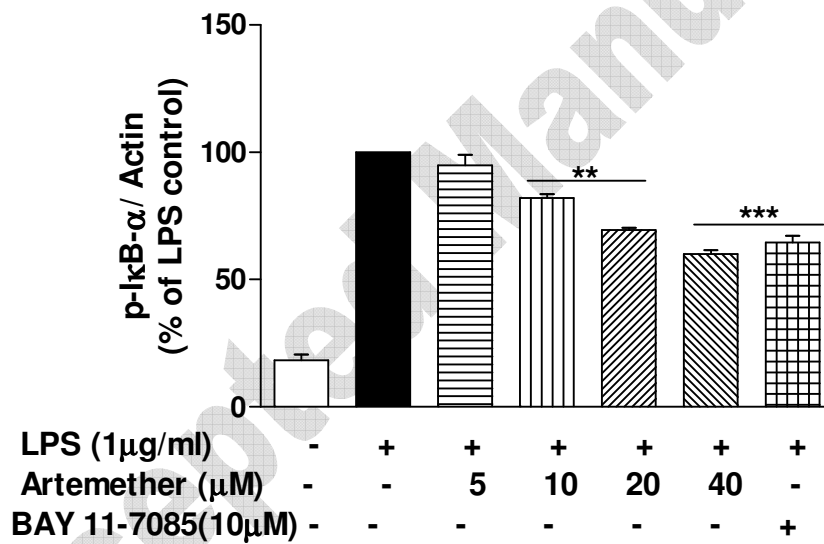
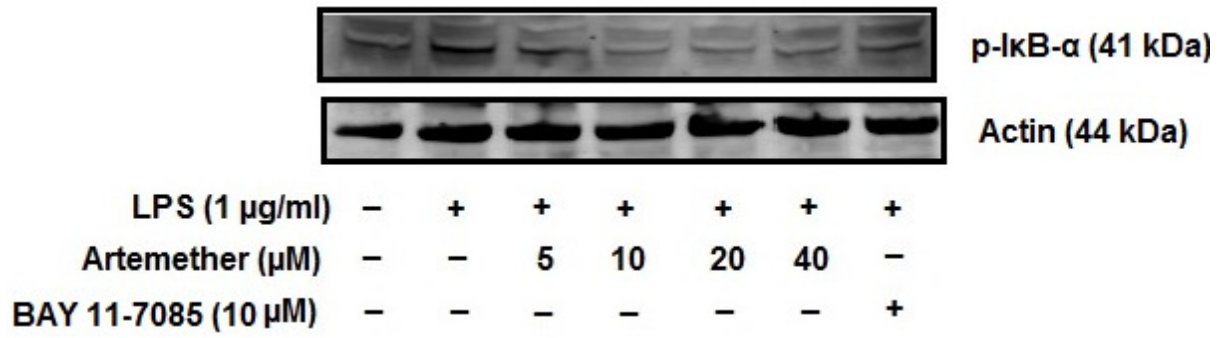


Figure 6c

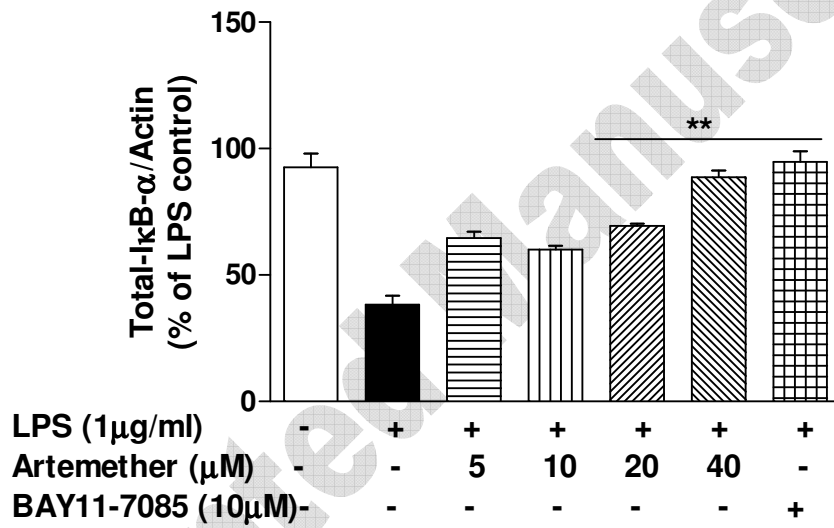
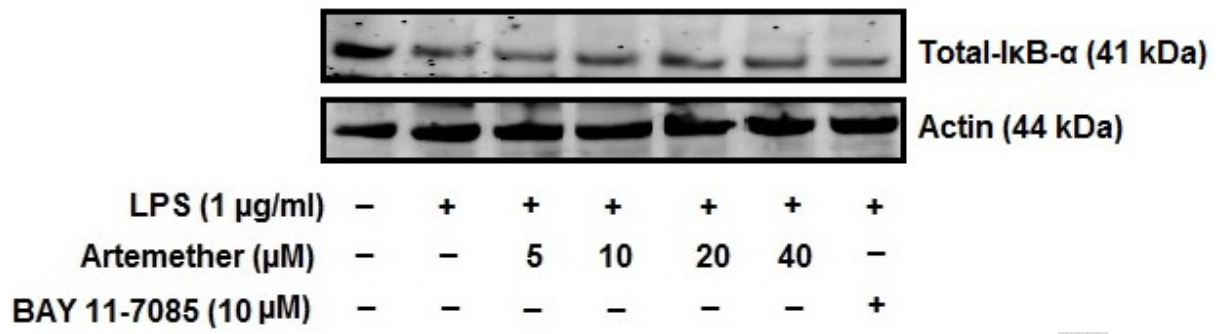


Figure 6d

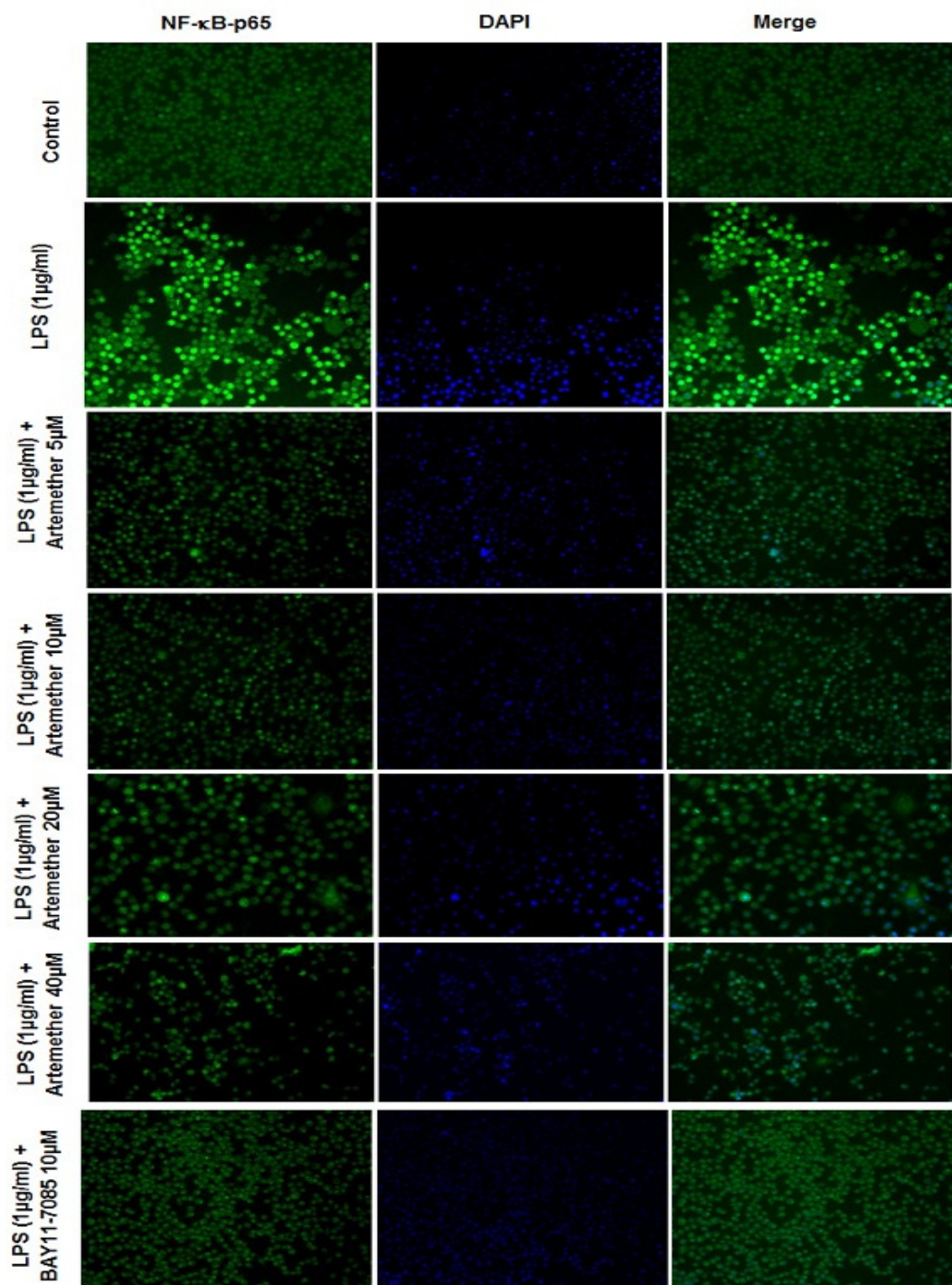
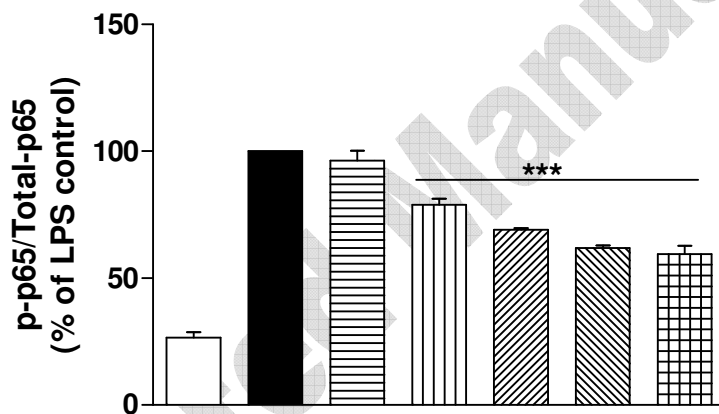
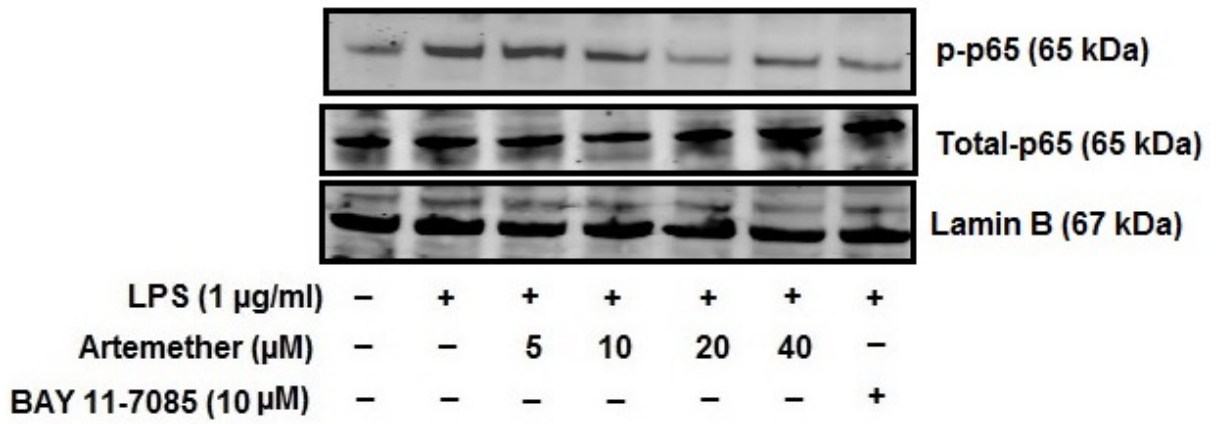


Figure 6e



LPS (1 µg/ml)	-	+	+	+	+	+	+
Artemether (µM)	-	-	5	10	20	40	-
BAY 11-7085 (10 µM)	-	-	-	-	-	-	+

Figure 6f

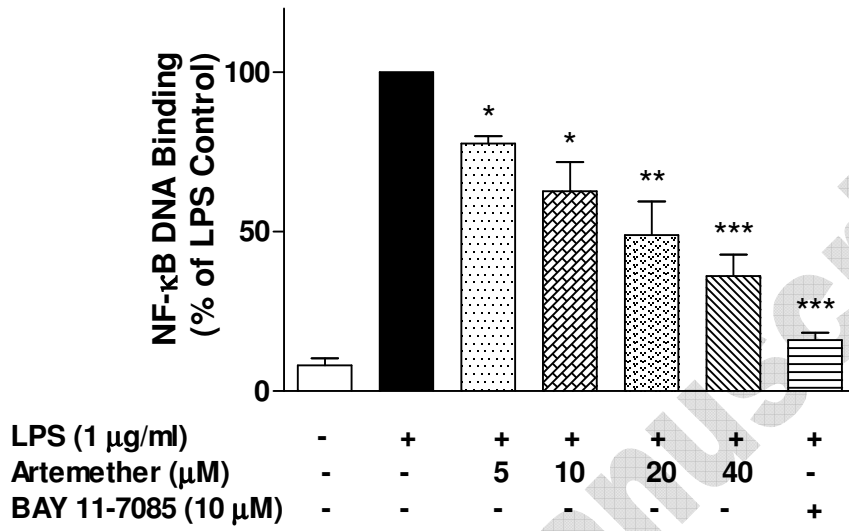


Figure 7a

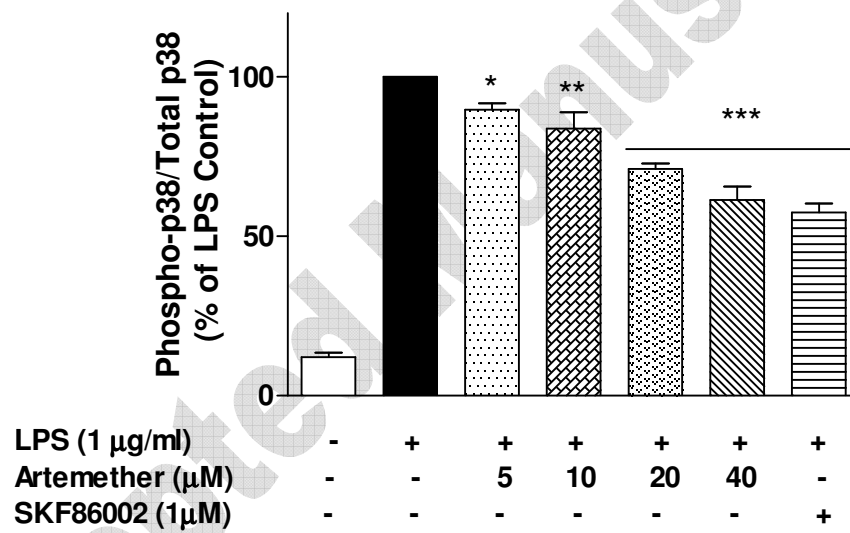
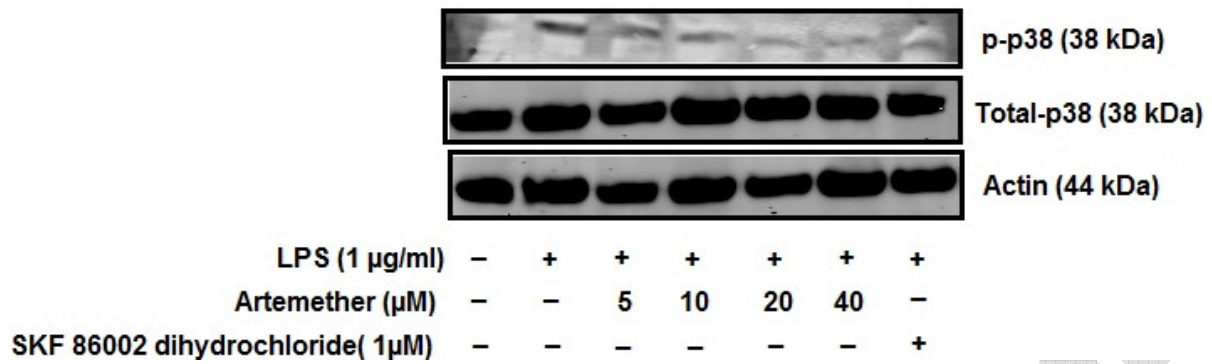


Figure 7b

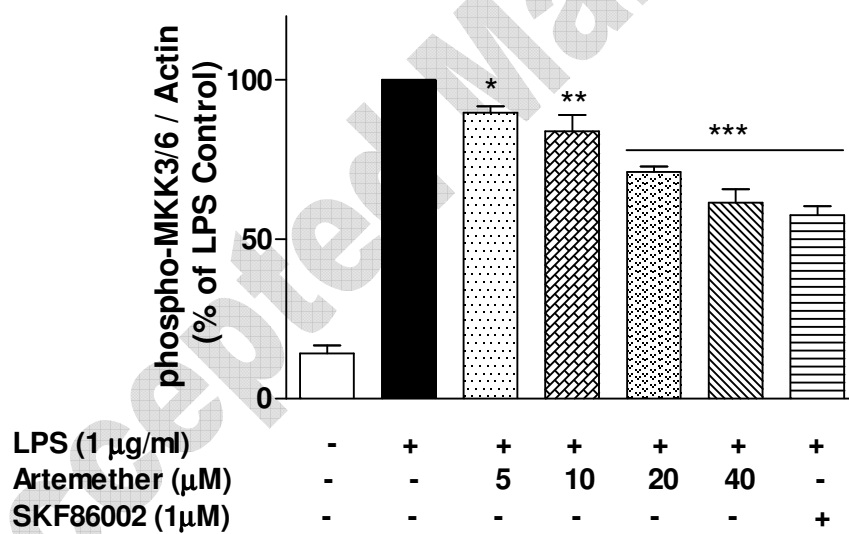
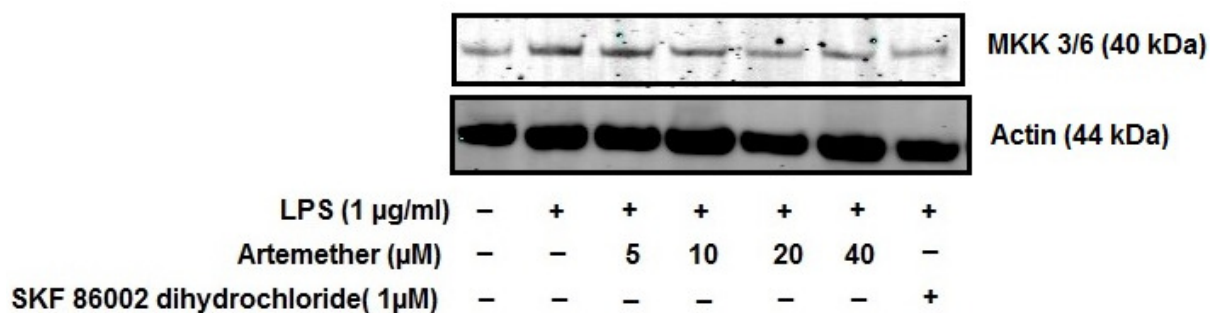
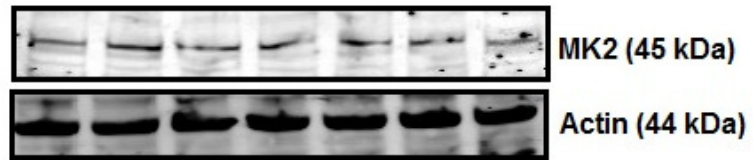
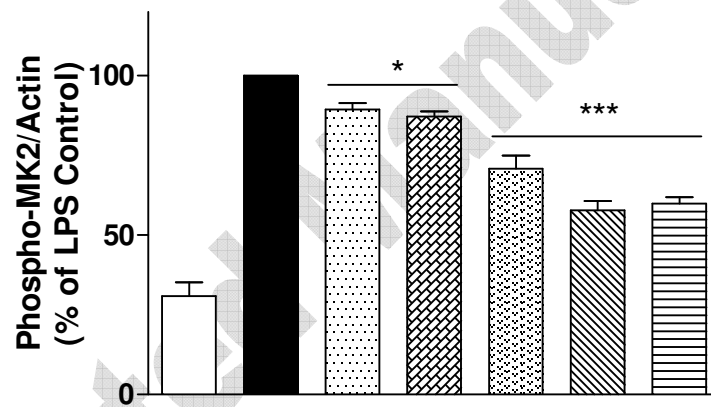


Figure 7c



LPS (1 µg/ml)	-	+	+	+	+	+	+
Artemether (µM)	-	-	5	10	20	40	-
SKF 86002 dihydrochloride( 1µM)	-	-	-	-	-	-	+



LPS (1 µg/ml)	-	+	+	+	+	+	+
Artemether (µM)	-	-	5	10	20	40	-
SKF86002 (1µM)	-	-	-	-	-	-	+

Figure 8a

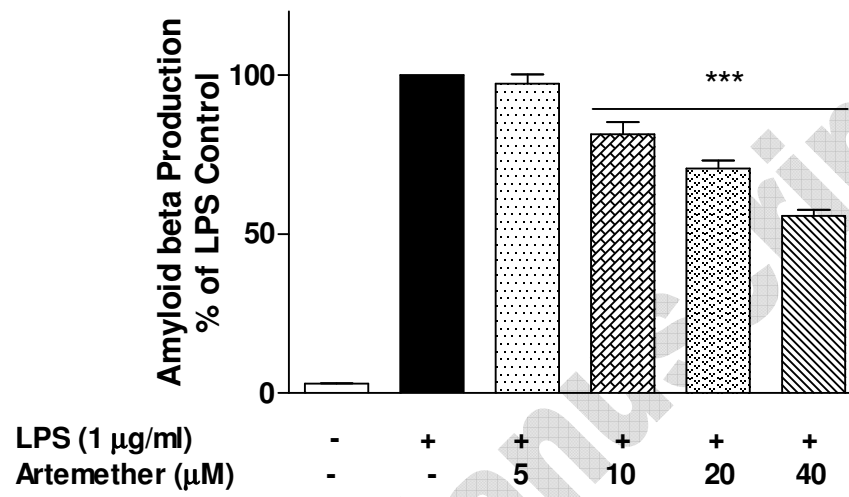
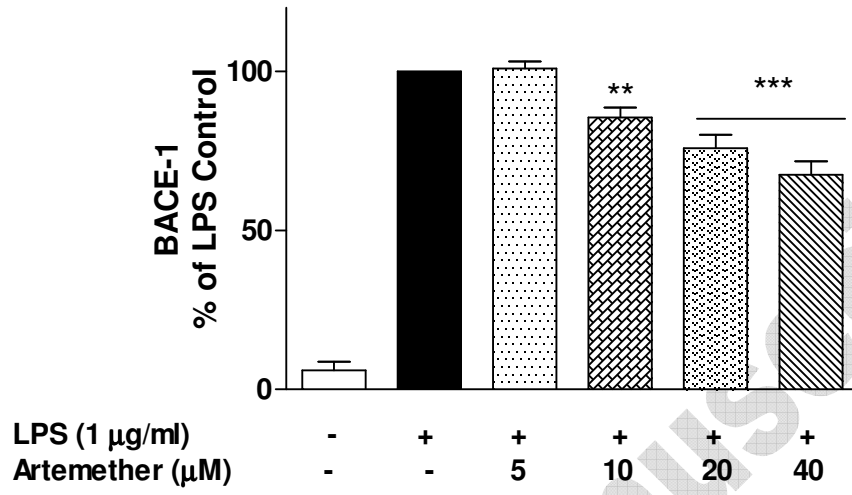


Figure 8b



Accepted Manuscript

Figure 9a

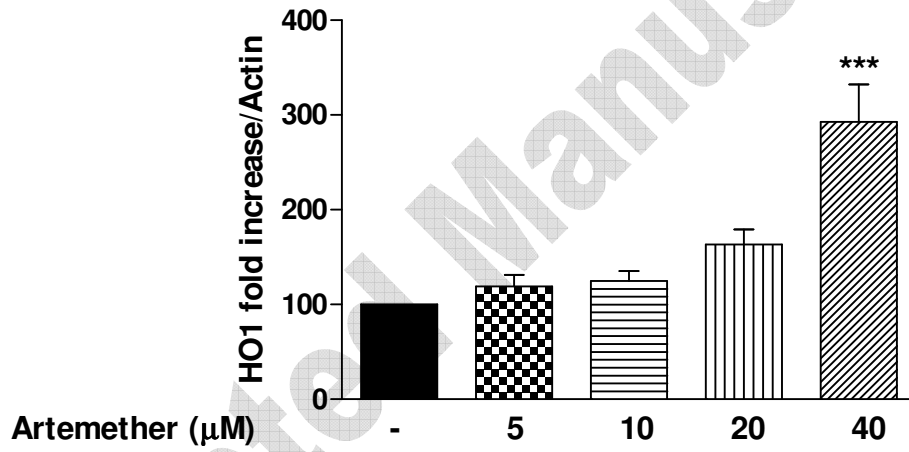
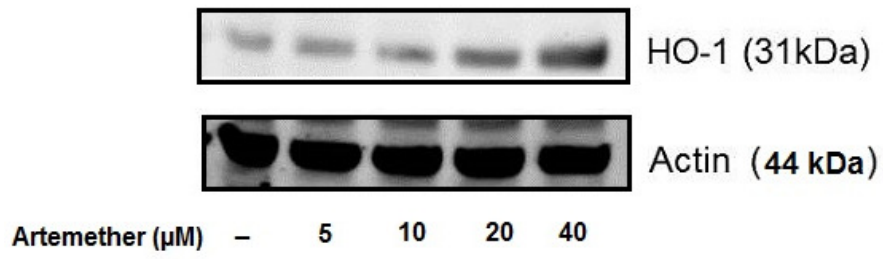


Figure 9b

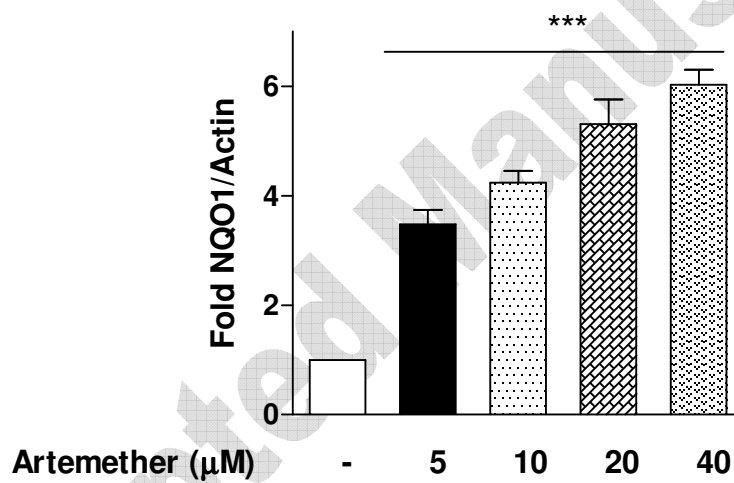
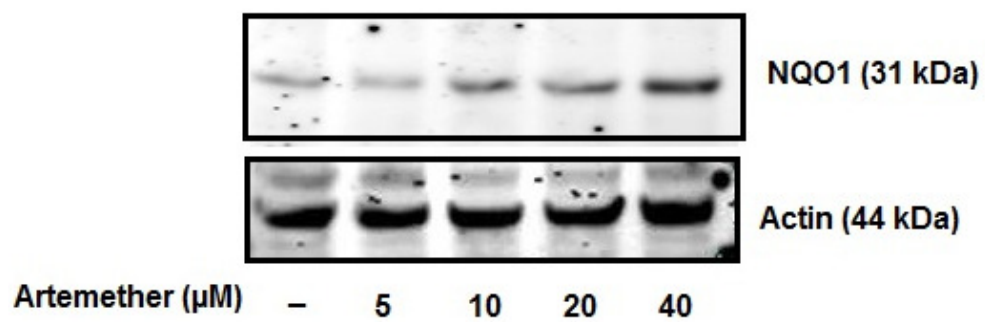
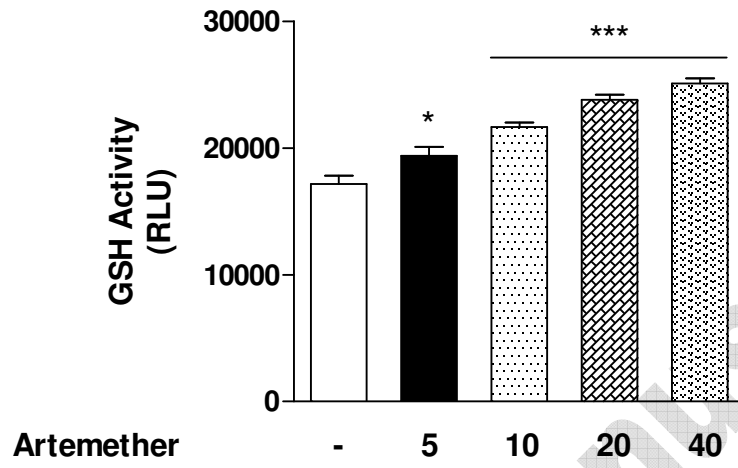
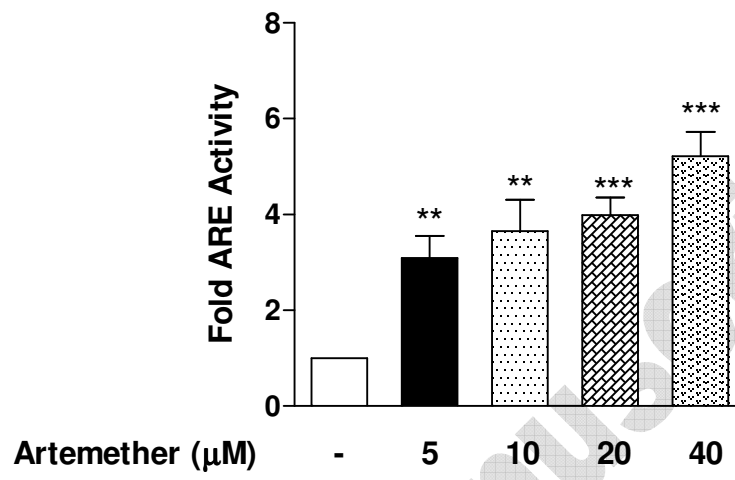


Figure 9c



Accepted Manuscript

Figure 9d



Accepted Manuscript

Figure 9e

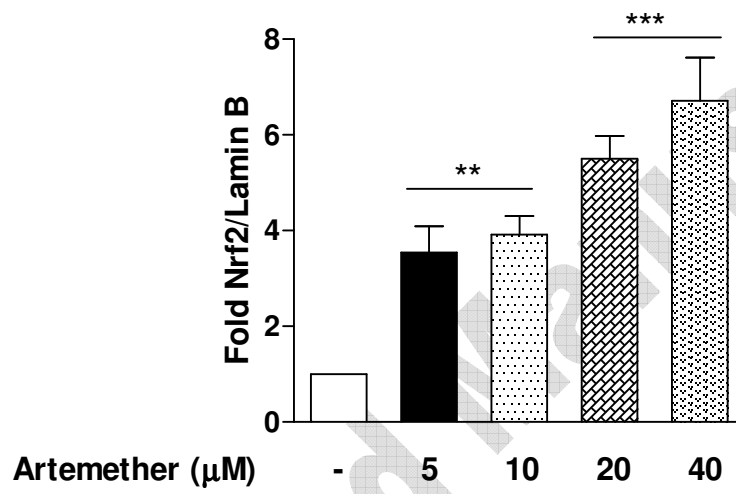
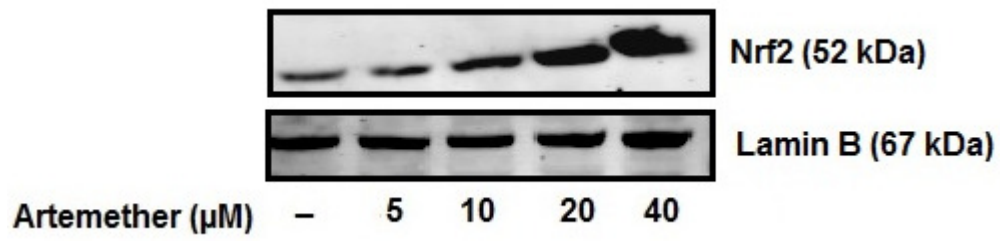


Figure 9f

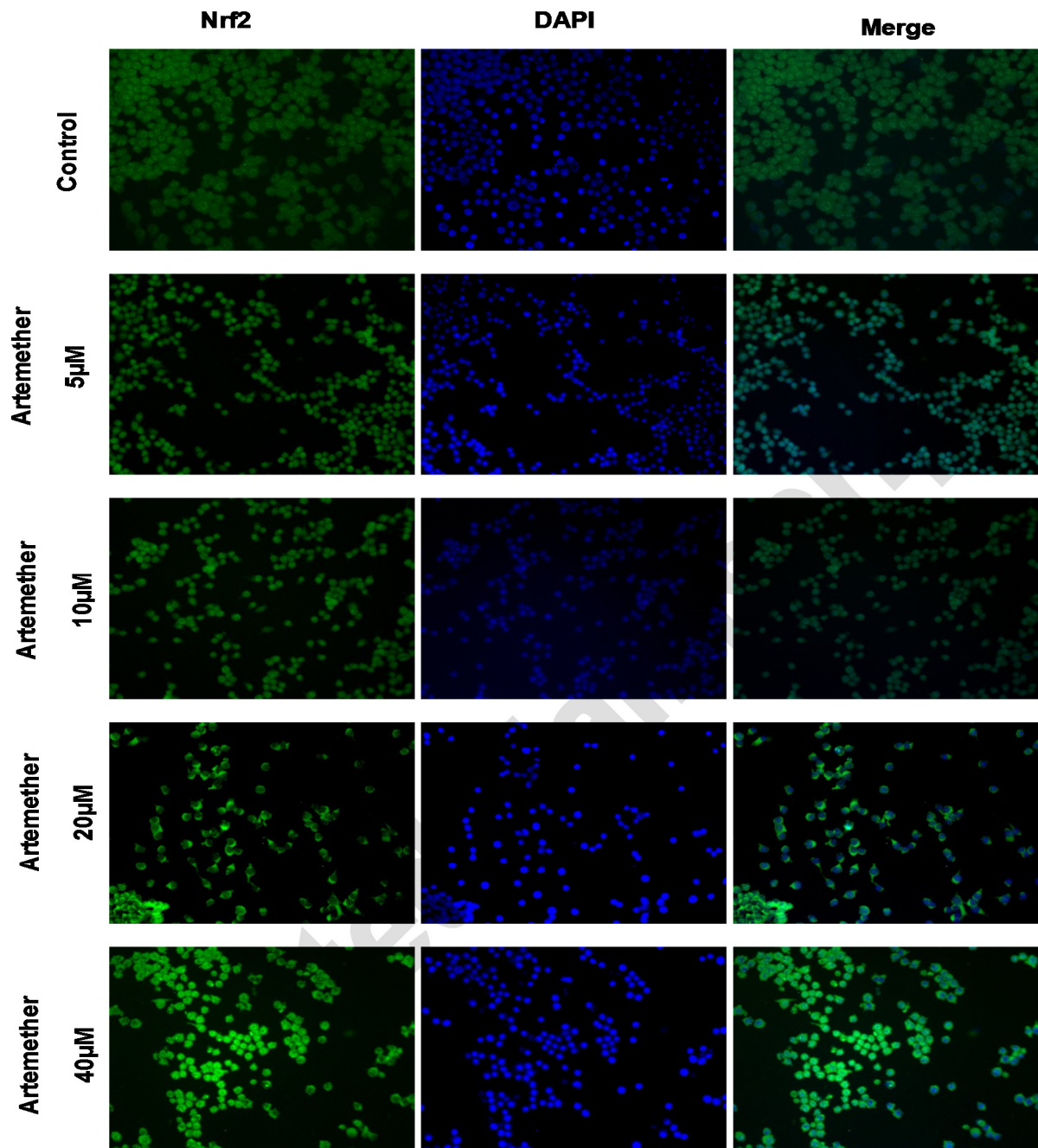


Figure 9g

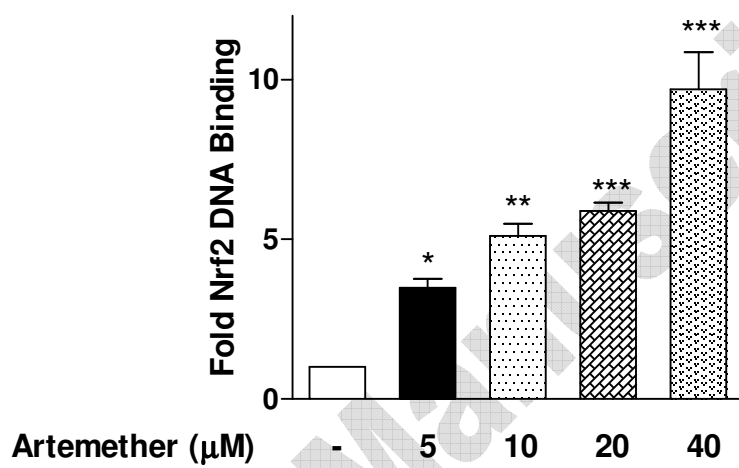
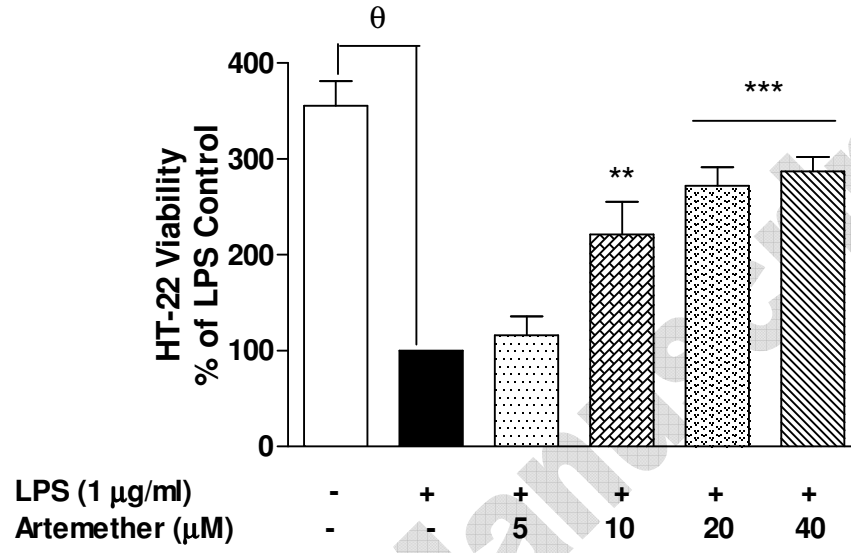


Figure 10a



Accepted Manuscript

Figure 10b

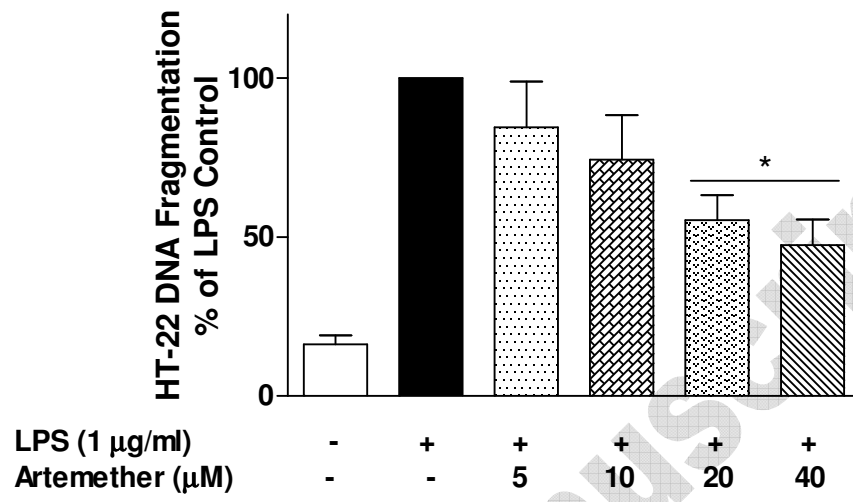
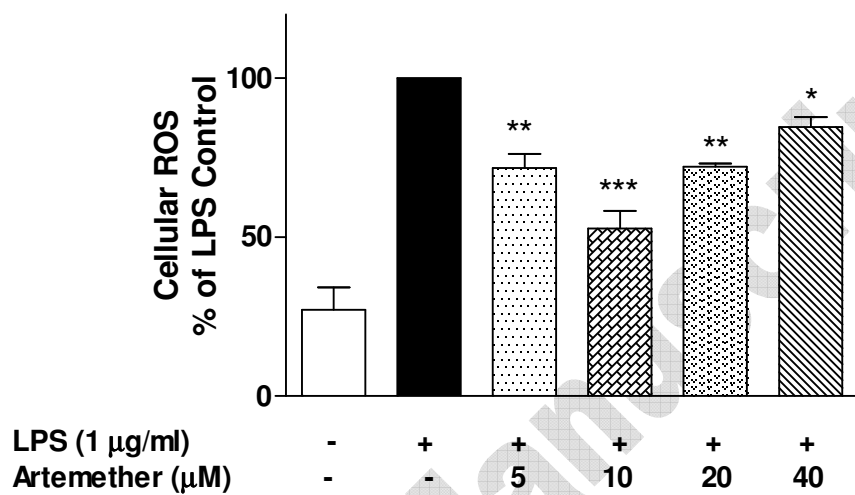


Figure 10c



Accepted Manuscript

Figure 11a

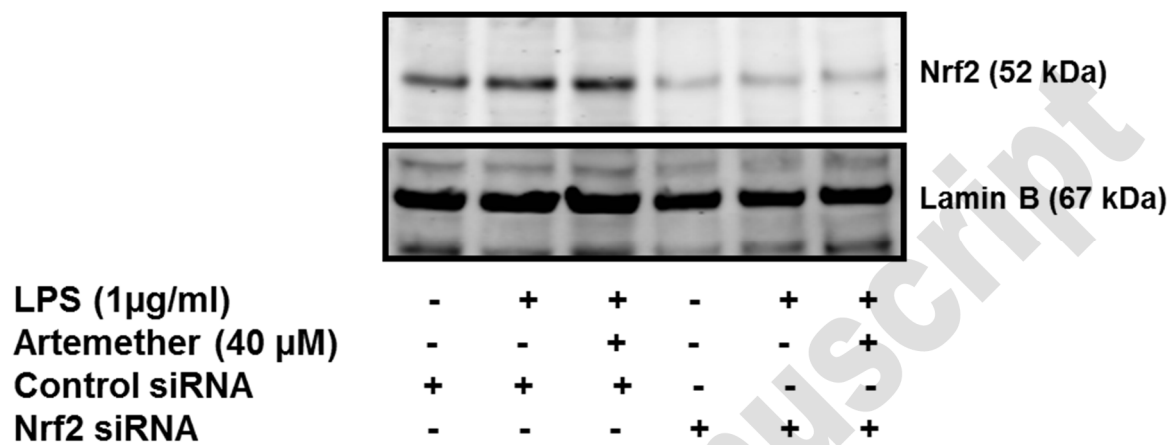
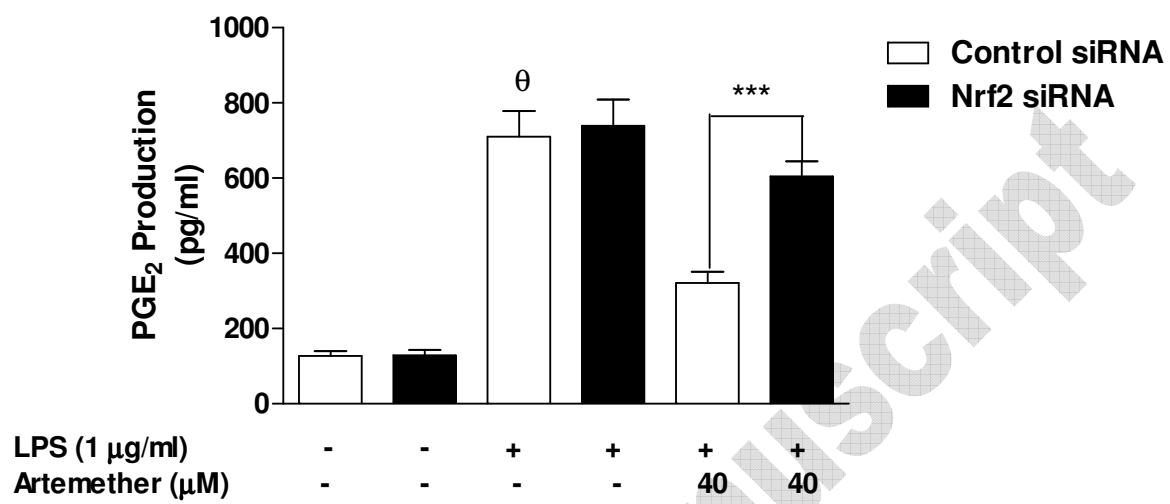
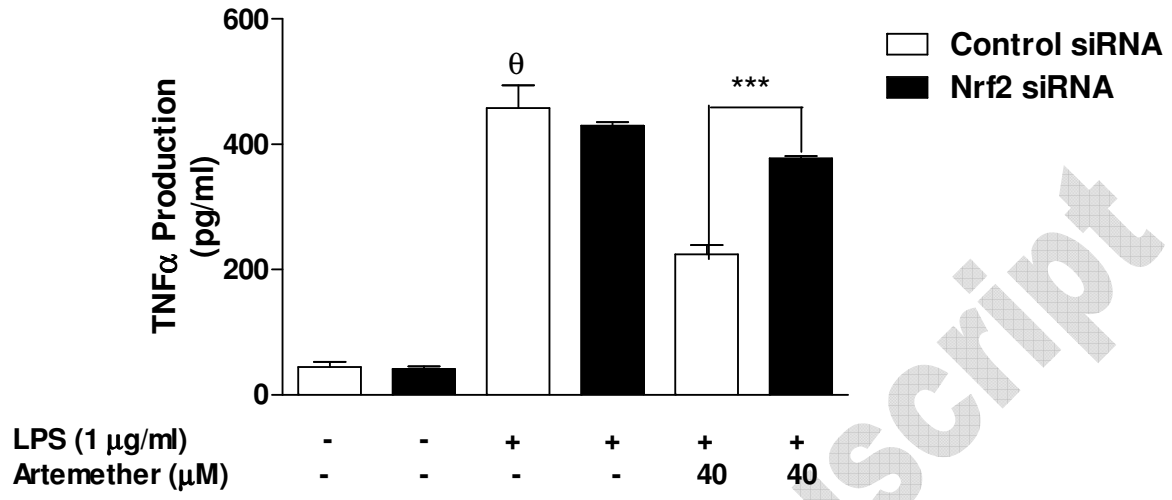


Figure 11b



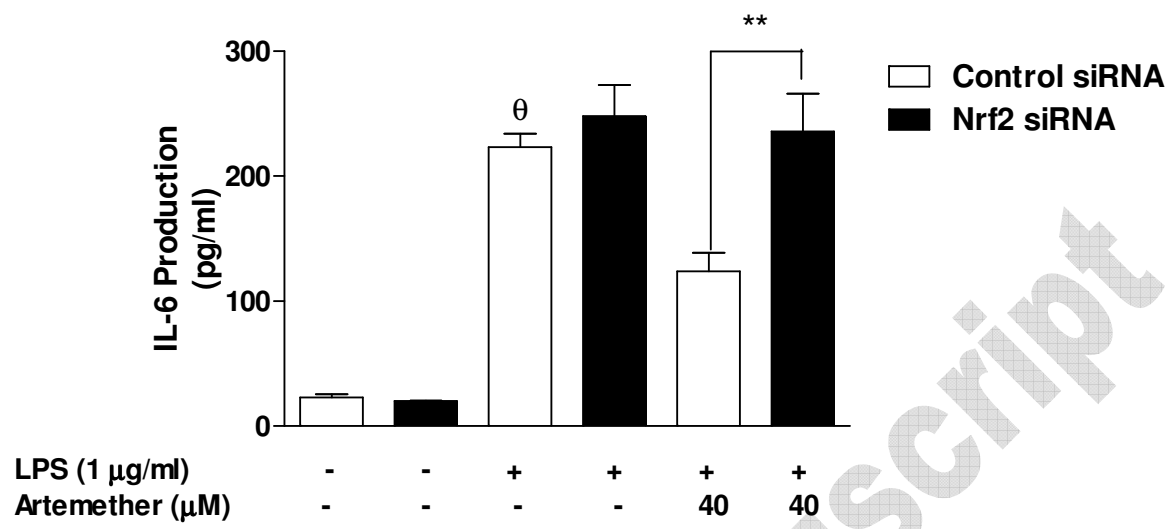
Accepted Manuscript

Figure 11c



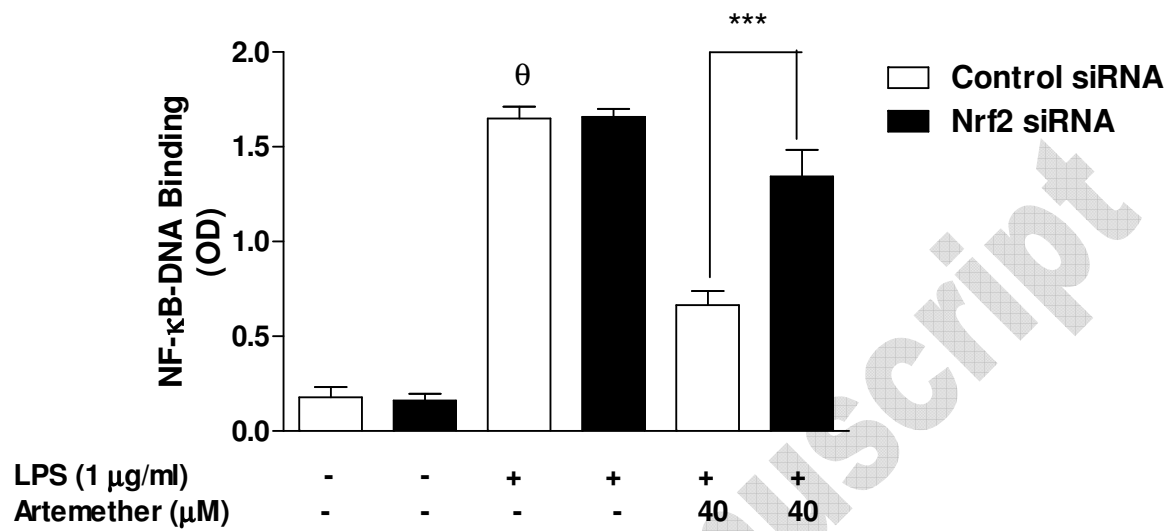
Accepted Manuscript

Figure 11d



Accepted Manuscript

Figure 11e



Accepted Manuscript

Figure 12a

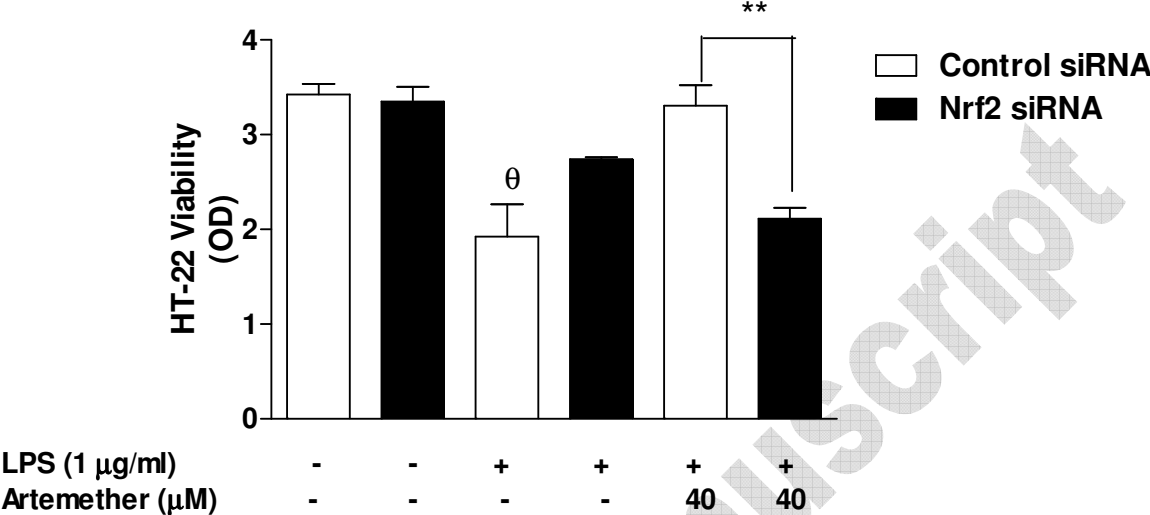
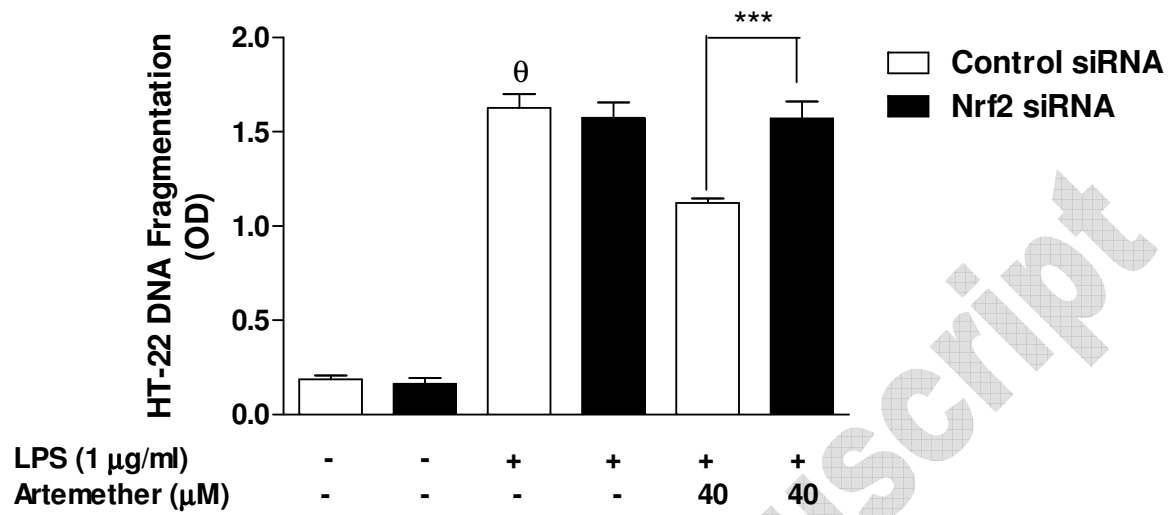


Figure 12b



Accepted Manuscript